Brief disruption of activity in a subset of dopaminergic neurons during consolidation impairs long-term memory by fragmenting sleep

Lin Yan[1,2,3], Litao Wu[1,2], Timothy D. Wiggin[4], Xiaojuan Su[1,2], Wei Yan[1,2], Hailiang Li[5], Lei Li[1,2], Zhonghua Lu[1,2], Yuantao Li[3], Zhiqiang Meng[1,2,6], Fang Guo[5], Fan Li[7*], Leslie C. Griffith[4*], Chang Liu[1,2*]

[1] Shenzhen-Hong Kong Institute of Brain Science, Shenzhen Institute of Advanced Technology, Chinese Academy of Sciences, Shenzhen, 518000, China

[2] CAS Key Laboratory of Brain Connectome and Manipulation, Shenzhen Institute of Advanced Technology, Chinese Academy of Sciences, Shenzhen, 518000, China

[3] Department of Anesthesiology, Shenzhen Maternity and Child Healthcare Hospital, Shenzhen, 518028, China

[4] Department of Biology, Volen National Center for Complex Systems, Brandeis University, Waltham, MA 02454-9110, USA

[5] School of Brain Science and Brain Medicine, Zhejiang University, Hangzhou, 310058, China

[6] Shenzhen Key Laboratory of Drug Addiction, Shenzhen Institute of Advanced Technology, Chinese Academy of Sciences, Shenzhen 518000, China

[7] Department of Pathophysiology, Shantou University Medical College, Shantou, 515041, China

[*] Corresponding authors names and email addresses:

Fan Li, lifan@stu.edu.cn

Leslie C. Griffith, griffith@brandeis.edu

Chang Liu, chang.liu3@siat.ac.cn

Abstract

Sleep disturbances are associated with poor long-term memory (LTM) formation, yet the underlying cell types and neural circuits involved have not been fully decoded. Dopamine neurons (DANs) are involved in memory processing at multiple stages. Here, using both male and female flies, *Drosophila melanogaster*, we show that, during the first few hours of memory consolidation, disruption of basal activity of a small subset of protocerebral anterior medial DANs (PAM-DANs), by either brief activation or inhibition of the two dorsal posterior medial (DPM) neurons, impairs 24 h LTM. Interestingly, these brief changes in activity using female flies result in sleep loss and fragmentation, especially at night. Pharmacological rescue of sleep after manipulation restores LTM. A specific subset of PAM-DANs (PAM-α1) that synapse onto DPM neurons specify the microcircuit that links sleep and memory. PAM-DANs, including PAM-α1, form functional synapses onto DPM mainly via multiple dopamine receptor subtypes. This PAM-α1 to DPM microcircuit exhibits a synchronized, transient, post-training increase in activity during the critical memory consolidation window, suggesting an effect of this microcircuit on maintaining the sleep necessary for LTM consolidation. Our results provide a new cellular and circuit basis for the complex relationship between sleep and memory.

Introduction

Memory consolidation is a time-dependent process which, during the immediate post-encoding period, facilitates maturation of newly formed but unstable memories (McGaugh, 2000; Dudai et al., 2015). Neurons undergo a cascade of events that actively remodel the connections at both synaptic and system levels to consolidate newly formed memories (Tonegawa et al., 2018). Systems consolidation, referring to the biological interaction between brain regions or circuits, results in establishment of an information flow for the neuronal ensemble during memory transformation (Dubnau and Chiang, 2013). Sleep, as one of the most important physiological processes that affects memory, has been shown to influence several different memory stages. Sleep deprivation (SD) before training compromises memory formation, while SD post-learning impairs memory consolidation (Li et al., 2009; Spira et al., 2014; Dag et al., 2019). The neural replay of memories during sleep, in particular, has been considered to be part of the active process of memory consolidation (Klinzing et al., 2019). However, the neural mechanisms that bridge sleep and memory consolidation are still largely unclear.

The fruit fly *Drosophila melanogaster* has proven to be a valuable model for uncovering the mechanistic underpinnings of memory formation, and studies in this organism have contributed to revealing the nature of the representations of memory traces formed in associative conditioning paradigms (Aso and Rubin, 2020; Adel, 2021). Classical olfactory conditioning, which stems from studies on Pavlov's dogs (Pavlov, 1927), forms a memory of a conditioned stimulus (CS, an odour) as a

pleasant or an unpleasant prediction of an unconditioned stimulus (US, a reward or a punishment) after pairing the CS with the US (Quinn, 1974; Tempel, 1983; Tully, 1985). Multiple types of neurons have been identified involved in distinct memory processes. Dopamine neurons (DANs), as an indispensable part of the US pathway, convey reinforcement signals to spatially segregated subdomains of the mushroom body (MB) to form appetitive or aversive short-term memories (STM) (Aso et al., 2012; Burke et al., 2012; Liu et al., 2012). In addition to their role in STM formation, DANs also participate in different phases of LTM (Placais et al., 2012). Different subsets of DANs are morphologically and functionally distinct (Mao and Davis, 2009; Aso et al., 2014a). Persistent activity in PPL1-γ1pedc and -γ2α'1 subtypes interferes with STM and anesthesia-resistant memory (ARM), and promotes forgetting (Berry et al., 2012; Placais et al., 2012; Berry et al., 2015), while PPL1-α2α'2 and PPL1-α3 mediate aversive LTM formation with persistent post-training activity (Feng et al., 2021). Delayed post-training activity in aSP13-DANs is required for LTM consolidation of courtship learning (Kruttner et al., 2015). The function of many of other subsets remains uncharacterized.

The MB, a multi-functional unit roughly analogous to the hippocampus in mammals, encodes and integrates CS and the US information in a compartmentalized manner. Dopamine (DA) released from DANs acts directly on the MB intrinsic neurons via D1-type receptors (Kim et al., 2007; Qin et al., 2012). Functional observations revealed that ongoing activity in α'β' neurons is required to maintain

memory during the first hour after training (Krashes et al., 2007). In addition, MB αβ core neurons have been shown to act as a gate to permit LTM consolidation (Huang et al., 2012). These data imply that during memory consolidation, a DA signal cascade recruits multiple subsets of neurons to exert sequential modulation of these functional loops. Additional processing takes place via activation of two pairs of extrinsic neurons, dorsal paired medial (DPM) neurons and anterior paired lateral (APL) neurons, which have been well characterized for their requirement in memory consolidation (Waddell, 2000; Keene et al., 2004; Keene et al., 2006; Zhang et al., 2013). In addition to memory processes, DA also regulates wakefulness and sleep by acting on distinct downstream targets (Kume et al., 2005; Donlea, 2011; Van Swinderen and Andretic, 2011; Ueno et al., 2012; Tomita et al., 2021). Subsets of PAM-DANs have been suggested to signal wakefulness and project to wake-promoting compartments of the MB (Sitaraman et al., 2015; Driscoll et al., 2021). Furthermore, DPM neurons have been shown to promote sleep via inhibitory signaling (Haynes et al., 2015). The role of the activity of DAN-DPM connections in consolidation has not been explored.

In this study, we show that PAM neurons form inhibitory connections on DPM neurons. Interestingly, activation of PAM neurons or inactivation of DPM neurons during the first few hours of memory consolidation results in an impairment of LTM. Furthermore, we observed a sleep reduction and fragmentation after brief disruption of these neurons. Finally, we identified a specific subset of PAM neurons that are

sufficient and necessary to modulate memory consolidation via sleep regulation, and characterized their functional connection with DPM neurons. Maintenance of basal activity of this specific microcircuit during memory consolidation has a profound effect on LTM, through influencing sleep in an internal state-dependent manner.

Results

PAM neurons form functional synapses and inhibit downstream DPM neurons

PAM neurons project to the horizontal lobes of the MB where they participate in formation of appetitive memory (Burke et al., 2012; Liu et al., 2012) (Figure 1A), and a pair of DPM neurons intensively innervates all lobes of the MB and is important for consolidation of memory (Yu et al., 2005; Keene et al., 2006) (Figure 1A). The electron microscope (EM) connectome database have shown the synaptic connection from PAM to DPM neurons with 4709 synapses (Zheng et al., 2018; Scheffer et al., 2020; Plaza et al., 2022). To determine if PAM and DPM neurons sequentially function together to regulate distinct memory processes, we first needed to determine how they were connected. We investigated the connectome-predicted structural and functional connection between PAM and DPM neurons using GFP Reconstitution Across Synaptic Partners (GRASP) and activity-dependent GRASP (Feinberg et al., 2008; Macpherson et al., 2015). Signals from GRASP and active GRASP, which detect physical proximity of neurons, were detected in the horizontal lobes of the MB in flies with split-GFP fragments (spGFP1-10/syb::spGFP1-10 and CD4::spGFP11)

expressing in PAM neurons labeled by R58E02-GAL4 or -LexA and DPM neurons labeled by L0111-LexA or eyeless-GAL80;MB-GAL80;c316-GAL4, respectively, showing that PAM neurons likely to connect to DPM neurons functionally (Figure 1B). Further, using a restricted *trans*-Tango, a technique to probe the synaptic connections between GAL4-labeled upstream neurons and LexA-labeled targeted neurons (Sun et al., 2022), we confirmed that DPM neurons labeled by newly generated VT064246-LexA drivers are the downstream target of PAM neurons (Figure 1C-D).

To investigate the functional connection from PAM to DPM neurons, we expressed $P2X_2$ receptors in PAM neurons using R58E02-LexA, and GCaMP6f in the DPM neurons using VT064246-GAL4. As we previously described, the change in fluorescence over time as a ratio to the initial level using $\triangle F/F = (Fn-F_0)/F_0 \times 100\%$ was used for quantification (Liu et al., 2019). We found that direct activation of PAM neurons by bath application of ATP resulted in a strong decrease in calcium, consistent with inhibition of DPM activity (Figure 2A, see also Table 3). To understand which dopamine receptor mediates this inhibition, we knocked down different dopamine receptors in DPM neurons using VT046004-GAL4, and imaged EPAC in DPM, an indicator of cAMP levels, after application of dopamine. Knockdown of Dop1R1 receptors in DPM neurons significantly rescued the dopamine-induced decrease in cAMP (visualized as a decrease in EPAC FRET), whereas knockdown Dop1R2 or DopEcR trended to further increasing cAMP level

(Figure 2B, see also Table 3). These data suggest that dopamine released from PAM neurons acts on DPM via multiple receptor subtypes, which may modulate the neural activity in a complex way. Our observations suggested the hypothesis that PAM neurons may be involved in memory consolidation via a direct synaptic connection with DPM neurons.

PAM and DPM neurons both influence memory consolidation

To understand the biological function of the inhibitory connection from PAM to DPM neurons, we wanted to ask whether PAM and DPM neurons participate in distinct memory processes or whether they are part of a single pathway. We first confirmed their roles in learning or consolidation, employing an appetitive olfactory conditioning paradigm which is able to induce LTM with a single session of training (Krashes and Waddell, 2008). Consistent with our previous work, activation of PAM neurons expressing dTrpA1 (Hamada et al., 2008) driven by R58E02-GAL4 paired with an odour for 1 min in non-starved and starved flies was sufficient to induce immediate appetitive memory (Figure 3A, see also Table 3) (Liu et al., 2012). Blocking the PAM neurons during training using shibire^{ts1} (shi^{ts1}), which inhibits neuronal output at high temperature (Krashes et al., 2009), resulted in 24 h appetitive memory defects (Figure 3B, see also Table 1), which is consistent with previous findings (Yamagata et al., 2015). DPM neurons have been found an essential role in memory consolidation during a critical window for consolidation (Waddell, 2000; Yu et al., 2005; Keene et al., 2006; Cervantes-Sandoval and Davis, 2012). In accordance with the

aforementioned findings, inactivation of DPM neurons by shi^{ts1} at restrictive temperature of 32 °C for 2.5 h after training resulted in a 24 h memory deficit (Figure 3C-D, see also Table 1), but there was no effect on 24 h memory when they were blocked before and during training (Figure 3E, see also Table 1). Since PAM neurons can inhibit DPM neurons, we wondered whether PAM neurons participate in the consolidation process and used conditional activation/inactivation to probe their role. Activation of PAM neurons for 1 h after training resulted in an impairment of 24 h memory (Figure 3F, see also Table 1). Without activation, *R58E02-GAL4/UAS-dTrpA1* flies and their genetic controls formed normal 24 h memory (Figure 3G, see also Table 1). Blocking the PAM neuronal activity after training for 2.5 h failed to disrupt 24 h memory (Figure 3H, see also Table 1), suggesting that activity of PAM neurons is necessary in the consolidation window or that heterogeneity in the subsets of PAM neurons masks any phenotype.

Increased or decreased activity of PAM neurons results in reduced and fragmented sleep

It has been suggested that one of the important functions of DPM in consolidation is its ability to regulate sleep (Haynes et al., 2015). To understand whether the impairments in LTM that occurred with activation of PAM neurons after training were attributable to sleep disruption, we monitored sleep under starvation and normal feeding conditions before (LP1), during and 24 h after activation/inactivation (DP1 and LP2) using the Drosophila Activity Monitor (DAM2) System. We measured sleep

amount, the number of sleep episodes and P(wake), a parameter which reflects sleep depth (Liu et al., 2019; Wiggin et al., 2020). Sleep data were analyzed in one-hour bins to assess dynamic changes during the course of starvation before the time when training would have occurred through the time when the 24 h memory tests would have been done (Figure 4, see also Table 4). Activation/inactivation periods were applied in the same time windows that reliably disrupted LTM 1 h for the PAM neurons and 2.5 h for the DPM neurons, immediately after when training would have occurred.

A reduction in sleep occurred a few hours after activation of PAM neurons (Figure 4A, upper panel), possibly due to a reduced number of sleep episodes (Figure 4A, middle panel) and an increased possibility of waking (Figure 4A, lower panel). The biggest change, however, was structural- PAM activation significantly increased the number of sleep episodes, which reflects increased wakefulness during the dark period following activation (Figure 4A, middle panel). Although LTM impairment was similar in the memory experiments, the effect of inactivation of DPM neurons resulted in a slightly stronger, long-lasting sleep reduction and fragmentation that was delayed until the dark period after inactivation (Figure 4C-D). Unexpectedly, inactivation of PAM neurons led to a sleep change similar to that seen with inactivation of DPM neurons (Figure 4B), suggesting that perhaps a specific subsets of PAM neurons was important for linking memory consolidation and sleep via modulation of DPM. The weak effect of activation of the large R58E02-GAL4+

group of PAM neurons on sleep could be due to masking of the role of a PAM subgroup by inter-PAM interactions or DPM-independent effects on sleep.

Appetitive LTM expression requires that the animal be motivated by hunger (Liu et al., 2012) and starvation is known to suppresses sleep (MacFadyen, 1973; Keene et al., 2010; Thimgan et al. 2010). To determine whether the memory defect and sleep disruption are linked to a certain internal state, we also analyzed the sleep effects of manipulation of PAM and DPM neurons under a no starvation condition (Figure 5). Without starvation, activation of PAM neurons led to a significant decrease in total sleep during the activation period, and also to a significant reduction in the early night (Figure 5A, see also Table 4), suggesting a complex and context-dependent role for PAM neurons in regulation of sleep. Inactivation of PAM neurons (Figure 5B, see also Table 4), inactivation or activation DPM neurons (Figure 5C-D, see also Table 4) in the fed condition produced almost no change in sleep pattern compared to genetic controls before, during and after manipulation. Taken together, these observations again raise the possibility that there may be subtype-specific actions of PAM neurons on DPM neurons. They also demonstrate that their interactions are likely to be context-dependent.

The PAM-α1 subset of PAM neurons contributes to linking memory consolidation and sleep

The PAM neurons signaling reward for STM and LTM have been shown to be distinct groups that can be labeled separately by R48B04-GAL4 and R15A04-GAL4,

except for overlapping expression in the neurons projecting to the γ5 subdomain (Yamagata et al., 2015). Terminals of R15A04-GAL4 labeling (LTM-PAM) neurons are localized in the β2, α1, β'1, γ5 and pedunculus MB subdomains (Figure 6A). Terminals of R48B04-GAL4 labeling (STM-PAM) neurons are localized in the β'2, β1, and γ1-5 MB subdomains (Figure 6C). To address which subsets of PAM neurons are involved in the process of consolidation, we employed the same single session of appetitive conditioning protocol, activated these neurons after training for 1 h, and examined their 24 h memory. We found that activation of LTM-PAM neurons impaired 24 h memory (Figure 6B, see also Table 1). In contrast, activation of STM-PAM neurons did not affect 24 h memory (Figure 6D, see also Table 1). Thus, LTM-PAM neurons participate in the process of memory consolidation.

To identify which subset(s) of LTM-PAM neurons are involved in the regulation of memory consolidation, we tested split-GAL4 drivers labeling more specific groups. MB213B-, MB025B-, MB032B- and MB315C-GAL4+ neurons innervate to β1/β2, β'1, β'2 and γ5 subdomains, respectively (Figure 6E). We trained flies expressing dTrpA1 under control of each of these drivers, +/- 1 h activation after training, and tested 24 h memory. Only activation of MB299B-GAL4+ and MB043B-GAL4+ neurons impaired 24 h memory compared to their no-activation groups (Figure 6F, see also Table 2). MB299B-GAL4+ (which labels 12±5 PAM neurons/hemisphere) and MB043B-GAL4+ (which labels 6±2 PAM neurons/hemisphere) primarily label the α1

subdomain (Figure 6G). These data indicate that elevated activity of PAM-α1 neurons during consolidation impedes LTM.

To further probe the requirement of PAM-α1 neurons in memory consolidation, we either activated PAM-α1 neurons or blocked the output of PAM-α1 neurons for 1 h or 2.5 h after training, and tested 24 h memory of the experimental flies along with their genetic controls. Activation of both MB299B-GAL4 and MB043B-GAL4 labelled PAM-α1 neurons resulted in an impairment of 24 h memory (Figure 7A-B, see also Table 1). Blockade of MB299B-GAL4+, but not MB043B-GAL4+ neurons, also resulted in 24 h memory defect (Figure 7C-D, see also Table 1), perhaps reflecting a difference in the number or identity of the PAM-α1 neurons in each line (Figure 6G). Consistent finding was observed previously using MB299B (Ichinose et al., 2015; Chouhan et al., 2022). Interestingly, inactivation of the large group of R58E02+ PAM neurons (Figure 3H) also failed to impair 24 h LTM supporting the idea that the presence of additional non-α1 PAM neurons might suppress some phenotypes. The connectome catalogs both PAM to PAM connections and recurrent PAM to MBON network loops that might underlie some of the differences between these GAL4 lines.

PAM-α1 neurons have been shown to be important for LTM formation, memory retention and updating memory (Huetteroth et al., 2015; Ichinose et al., 2015; Aso and Rubin, 2016; Yamagata et al., 2016). To clarify if their action is specific to consolidation or to forgetting or retrieval, we activated and/or blocked PAM-α1

neurons labeled by MB299B-GAL4 prior to and or during the 24 h memory test. Activation of PAM-α1 prior to retrieval impaired 24 h memory (Figure 7E, see also Table 1), but activation and inactivation of PAM-α1 neurons during retrieval did not affect 24 h memory (Figure 7F-G, see also Table 1). These data suggest that PAM-α1 neurons may interact with the active forgetting process during a specific window, but they are not required for retrieval. In aggregate, our findings indicate that the normal activity of PAM-α1 neurons after training is critical to maintain the processing of memory consolidation.

To investigate whether 24 h memory defects were attributable to disrupted sleep secondary to changes in activity of PAM-α1 neurons, we recorded and analyzed sleep. Neither activation nor inactivation in fed flies had a major effect on sleep (Figure 8A-D, see also Table 4). Consistent with a context-regulated role in linking sleep and memory, activation of PAM-α1 neurons labeled by MB299B and MB043B under starvation conditions reduced sleep amount mainly during DP1 (Figure 7H, 7J, upper panel, see also Table 4), reminiscent of DPM suppression. The night after activation of PAM-α1 neurons, flies exhibited a significantly increased number of sleep episodes and P(wake) (Figure 7H, 7J, middle and lower panels, see also Table 4). Inactivation of starved MB299B neurons had little effect on sleep, but inactivation of PAM-α1 labeled by MB043B produced a strong reduction and fragmentation of sleep under starvation (Figure 7I, 7K, see also Table 4), again suggesting effects of the differences in cell number/identity between the two drivers. In aggregate, these data demonstrate

that both brief increases and brief decreases in activity of PAM-α1 neurons can reduce and fragment sleep. The 24 h memory defect resulting from this change of PAM-α1 activity during consolidation is possibly due to a delayed effect on nighttime sleep, and is completely dependent on internal starvation status.

A specific PAM-α1-DPM inhibitory microcircuit binds memory consolidation and sleep via maintaining basal activity post-learning

Using a broadly-expressing driver that captures most if not all PAM neurons, we showed that PAM-DANs form inhibitory synapses onto the DPM neurons (Figure 1). To determine if the connections between the PAM-α1 subset and DPM neurons follow the same rules as the aggregate, we determined the connectivity of this subset. From the EM connectome database (Zheng et al., 2018; Scheffer et al., 2020) and analysis of the connectivity with NeuPrint (Plaza et al., 2022), we found that 14 PAM-α1 neurons of the right hemisphere form 11, 12, 13, 12, 16, 16, 12, 17, 21 and 17 synapses with the right DPM neuron, 5 out of 14 PAM-α1 neurons form a single synapse and one PAM-α1 neuron form 4 synapses with the left DPM neuron, based on the Hemibrain connectome dataset (Figure 9A).To determine the functional connection between PAM-α1 and DPM neurons, we expressed $P2X_2$, ATP receptors in PAM-α1 neurons labeled by MB299B and GCaMP6f in the DPM neurons using VT064246-LexA (III), respectively, and confirmed an inhibition from PAM-α1 to DPM neurons by observing a significant decrease in GCaMP signal after application of ATP *in vitro* (Figure 9B, see also Table 3).

We also wanted to know if PAM-α1 and DPM activity changed post-learning, so we employed a newly developed tool, CREB-regulated transcriptional co-activator (CRTC) (Bonheur et al., 2023), to capture neural activity specifically during the critical consolidation window. Activity drives CRTC::GFP into the nucleus on a minute time scale, allowing visualization of recent activity by measurement of nuclear GFP levels. Subcellular distribution of CRTC::GFP signal in the cell bodies of PAM-α1 and DPM neurons were evaluated under different conditions. GFP signals in the nucleus of PAM-α1 but not DPM neurons significantly increased under starvation (Figure 9D-E, see also Table 1), suggesting a state-dependent resetting of activity in PAM-α1 neurons. Compared to the untrained group, we observed higher activity in both PAM-α1 and DPM neurons right after training (Figure 9C-E, see also Table 3). At 1 h of post-training, neural activity of PAM-α1 and DPM neurons was statistically indistinguishable from their untrained group; in the case of DPM it was significantly decreased compared to the timepoint of right after training, in the case of PAM-α1 the decrease was not statistically significant (Figure 9C-E, see also Table 3). These data suggest that the PAM-α1-DPM microcircuit exhibits synchronized neural activity changes during the consolidation window, and this may allow natural memory processes and sleep to be yoked. The fact that both increases and decreases of PAM-α1 activity break this synergy argues that the starvation-dependent resetting of PAM-α1 activity level is a critical feature of the state-dependent function of this circuit.

While it is clear that these two neuron types are connected, it was still possible that they function in sleep and LTM via parallel, independent pathways. If this was true, we would predict that the effects of inactivating both neuron groups at the same time should additively decrease sleep. To determine if this was the case, we simultaneously inactivated these neurons by expressing shi^{ts1} in both cell groups, and found sleep reduction and fragmentation statistically the same as when each of them was inactivated separately under starvation (Figure 10A-B, see also Table 4). This result supports a model of a PAM-DPM microcircuit which link sleep and memory consolidation.

Lastly, to cement the link between sleep disruption by manipulation of this circuit and memory impairment, we employed a pharmacological method. Rescue of the sleep disturbance produced by activating PAM-α1 for an hour by feeding of gaboxadol (also called THIP), a GABA agonist that promotes sleep (Dissel et al., 2015) was sufficient to also rescue memory consolidation, as reflected by memory levels comparable to the genetic controls and significantly better than the no-THIP group (Figure 10C-E, see also Table 1, 2 and 4). Taken together, these results support a mechanistic link between PAM-α1-DPM microcircuit activity in the post-learning time window and both memory consolidation and sleep.

Discussion

PAM-DANs have been known to be important for formation of short-term and long-term memories, and DPM neurons for memory consolidation and sleep. In the present study as summarized in Figure 10F, we find that these two types of MB extrinsic neurons are connected by inhibitory synapses and play an essential role in bridging LTM stabilization via dynamic sleep change. We demonstrate that a brief disruption of this circuit, in particular of a subset of PAM neurons (PAM-α1) during the critical memory consolidation window, results in an impairment of LTM. Worth noticing, sleep loss and fragmentation occur hours after the brief disruption of this circuit when the flies are starved. Thus, maintenance of basal activity of PAM-α1-DPM microcircuit during memory consolidation has a profound effect on LTM, through influencing sleep when the animal is experiencing a certain internal state.

Mushroom body DANs are not just a valence signal

DANs can have multiple roles at different times in the memory process. PAM-α1 is one of many cell types of DANs that required for memory formation (Yamagata et al., 2015; Yamagata et al., 2021). We find that not only suppressed activity but also elevated activity of PAM-α1 neurons right after training can disrupt memory consolidation, supporting a role in consolidation (Ichinose et al., 2015). PAM-α1 neurons form a recurrent loop with MBON-α1 neurons (Aso et al., 2014b; Ichinose et al., 2015), and the recurrent DAN/MBON networks are likely to be important in many aspects of memory processing. Several subsets of DANs have been shown to be

involved in forgetting, PPL1-γ1pedc (MP1) and PPL1-γ2α'1 (MV1) for permanent forgetting (Berry et al., 2012), and PPL1-α2α'2 for transient forgetting (Sabandal et al., 2021). In addition, Aso and Rubin (2016) demonstrated that writing and updating memories recruit different rules across distinct MB compartments. Memory consolidation is a dynamic time window from hours after learning but may continue for weeks (Roesler and McGaugh, 2010), and many studies have suggested that sleep deprivation is important during memory consolidation but not retrieval (Krishnan et al., 2016; Manassero et al., 2022). Our results do not rule out a role for PAM-α1 in active forgetting processes, but it is clearly not required for retrieval (Figure 7E-G), adding a new layer of complexity of multiple functions within a single type of neurons.

Sleep interacts with mushroom body DANs in multiple ways

Sleep is thought to be indispensable to memory consolidation process, converting initially unstable memory into stable long-term memory during sleep (Diekelmann and Born, 2010; Klinzing et al., 2019; Girardeau and Lopes-Dos-Santos, 2021). Besides the amount of sleep, accumulating evidence have pointed out that sleep structure is responsible for memory processing (Rolls et al., 2011; Lipinska and Thomas, 2019; Liu et al., 2019; Kjaerby et al., 2022). In *Drosophila*, sleep structure can be evaluated by the number of sleep episodes as well as P(wake). The number of sleep episodes reflects the frequency of awakenings, and P(wake) is the probability of transitioning from a sleep to an awake state, that reflects as the threshold for arousal

(Liu et al., 2019; Wiggin et al., 2020). In the present study, we found that a brief disruption of neural activity of a specific microcircuit resulted in reduced and fragmented sleep, with a consequent impairment of LTM, providing a new circuit base for the linkage between these two processes.

DPM neurons process memory consolidation via promoting sleep, likely via GABA inhibition of wake-promoting MB-α'β' neurons (Donlea, 2011; Haynes et al., 2015), and this circuit also seems particularly important for consolidation (Krashes et al., 2007). DPM neurons have been recently endowed with new functions, such as a gatekeeper for intrinsic coincidence time windows, and a bridge for mediating multisensory stimulus binding (Okray et al., 2023; Zeng et al., 2023), further revealing a compartmentalized specificity and plasticity of microcircuits. The PAM-α1-DPM microcircuit in the present work unlocks an upstream modulation of MB circuits for linking memory and sleep.

There are "forgetting" DANs (such as PPL1-γ2α'1) whose activity has been shown to be suppressed by sleep (Berry et al., 2015). This PPL1-γ2α'1 subset, and other MB DANs (including PAM-α1) have been identified as wake promoting neurons (Donlea, 2011; Sitaraman et al., 2015; Driscoll et al., 2021). Maybe this is one of the ways the recurrent network processes sleep. Perhaps the activation of PAM-α1 decreases sleep and that allows PPL1-γ2α'1 to cause forgetting. This is a model that could be tested in the future. In spite of the fact that MB circuits have been elegantly investigated, the leap from the microcircuit level to the systems scale

remains daunting, and how these circuits enable consolidation during sleep still needs further investigation.

Internal state dictates circuit configuration for consolidation

Internal state, like starvation, gates many of interactions through molecular mediators and neural circuits (Keene et al., 2010; McDonald, 2010; Lin et al., 2019; Yurgel et al., 2019). DANs contribute robustly in coordination of state-dependent behaviors, such as facilitating starvation-dependent sugar memory, and mediating starvation-driven food seeking behavior (Krashes et al., 2009; Tsao et al., 2018; Senapati et al., 2019). Driven by context, distinct subsets of DANs exhibit suppressed or enhanced neuronal responses facilitating integration of motivational signals and modulating output behaviors (Liu et al., 2017; Jovanoski et al., 2023). Our present study characterizes another subset of DANs that respond to starvation with an increase in neural activity to provide a context-dependent regulation of behavior. It is well known that starvation suppresses sleep (MacFadyen, 1973; Thimgan et al., 2010; Melnattur and Shaw, 2019), and sleep serves memory consolidation (Brodt et al., 2023; Chandra et al., 2023). Paradoxically, flies need to be starved to express appetitive LTM. But it can be interpretated in a way that the animal's state during consolidation can recruit different circuitry at both the KC level and the DAN level (Chouhan et al., 2021; Chouhan and Sehgal, 2022). Our results provides yet another example of this. Disrupted activity of PAM-α1-DPM microcircuit negatively impacts on both sleep and memory only when

the animal is starved. The activity of the microcircuit we have identified is likely to be key to understanding how sleep need is taken out of the loop during starvation.

An additional interesting feature of the role of PAM-α1 neurons in consolidation of appetitive LTM is that it is very sensitive to the level of activity within this neuron group (Figure 10E). Both increases and decreases in activity can block LTM and fragment sleep. The inhibitory nature of the connectivity between PAM-α1 and DPM provides a plausible explanation for the effects of overactivation of PAM-α1: strongly blocking DPM activity would suppress both sleep and consolidation (Waddell, 2000; Keene et al., 2004; Yu et al., 2005; Krashes and Waddell, 2008; Haynes et al., 2015). How inactivation of PAM-α1 produces a similar 'DPM-inhibition-like' state is more difficult to explain with current data. Whether this is a direct effect of decreasing the level of stimulation of dopamine receptors that occurs under starvation conditions when PAM-α1 activity increases (Figure 9D) or if it is an indirect effect mediated by an interneuron will require further investigation

Materials and methods

Animals

All flies were reared on standard cornmeal food at 25 □ and 60% relative humidity on a 12 h/12 h light-dark cycle. Flies expressing dTrpA1 and shi^{ts1} used in temperature-shift experiments were raised at 23 □. Flies for memory and sleep experiments allowed to freely mate. 5-10 days old and 5-7 days old adult flies were

used at the start of memory and sleep experiments, respectively. The following stocks were obtained from the Bloomington Drosophila stock center (BDSC, Indiana University): *w;;R58E02-GAL4* (70226), *w;;R15A04-GAL4* (48671), *w;;R48B04-GAL4* (50347) , *MB025B-GAL4* (68299), *MB213B-GAL4* (68273), *MB032B-GAL4* (68251), *MB315C-GAL4* (68316), *MB299B-GAL4* (68310), *MB043B-GAL4* (68304), *UAS-mCD8::GFP; Pin/Cyo* (5136) , *w;UAS-dTrpA1* (26263), *w;;UAS-shibire*^{ts1} (44222), *w;R58E02-LexA* (52740), *eyeless-GAL80;MB-GAL80/Cyo;c316-GAL4/TM6B* (30380), *UAS-CD8::RFP,LexAop-CD8::GFP* (302229), *LexAop-nSyb:spGFP1-10,UAS-CD4:spGFP11;MKRS/TM6B* (64315), *UAS-EPAC* (78802), *UAS-dcr2* (24650), *LexAop-P2X*$_2$ (76030), *UAS-GCaMP6f* (42747), *UAS-CD4-spGFP1-10* (93016), *LexAop-CD4-spGFP11* (93019), *UAS-DopEcR RNAi* (31981), *UAS-P2X*$_2$ (91223) and *LexAop-GCaMP6f* (44277), *UAS-CRTC::GFP/CyO; UAS-mCD8::mCherry-T2A-nls::LacZ in VK00005/TM2* (99656). *VT064246-GAL4/TM2* (v204311), *UAS-Dop1R1 RNAi* (v107058), *UAS-Dop1R2 RNAi* (v3392) were ordered from Vienna Drosophila Resource Center (VDRC, Vienna, Austria). *VT046004-GAL4* was one of Vienna Tile GAL4 lines, currently available at Korea *Drosophila* Resource Center (12772). The following lines have been previously described: *trans-Tango,QUAS-FLP;LexAop-FRT-RFP-FRT-GFP* (Sun et al., 2022). For behavioral experiments, *w*^{CS}*,UAS-dTrpA1* or *w;;UAS-shi*^{ts1} virgin female flies were

crossed to male flies of GAL4 lines. Virgin female w^{CS} flies were crossed with GAL4 or UAS parental lines as genetic controls.

The *VT064246-LexA* transgenic lines were based on VT064246-GAL4. The 2296 bp promotor fragment was amplified from genomic DNA of wild-type flies using the same primers as used for VT064246-GAL4 (forward primer: 5'-AATACGAGAGCGCTCACTAC-3' and reverse primer: 5'-TCTTATGGACGGCGA

GGAG-3'). This fragment was then cloned into enhancer-LexA vector (Fungene Biotech, http://www.fungene.tech) using NotI and AscI (Thermo Fisher Scientific) restriction sites. The sequence was confirmed by sequencing using primers as follow: VT064246-3F: 5'-AATACGAGAGCGCTCACTAC-3' and reverse lexA-5R: 5'-TCTTATGGACGGCGAGGAG-3'. The plasmids were inserted into attP40 (25C6 of chromosome 2) site and attP2 (68A4 of chromosome 3) site using attp PhiC31 mediated recombination (Fungene Biotech).

Memory assays

F1 generation of mixed genders in a group were trained and tested together. All training was carried out under the condition of dim red light and all tests were performed in darkness.

4-methylcyclohexanol (MCH) and 3-octanol (OCT) diluted in mineral oil to 10% were used as conditioned odours. Flies were trained with/without starvation. Flies

were starved for 30-46 h when each genotype exhibits a mortality rate of 10%-20% when flies started to be tested.

The paradigm to induce reward immediate memory by activation of rewarding DANs was performed as described previously (Liu et al., 2012). Briefly, a group of about 50 flies were loaded into the training tubes and accommodated for 1 min. Two odours were presented at 30 □ and 23 □ for 1 min reciprocally, and tested the choices between the two odours for 2 min. 30 □ was applied either with the first presented odour or the second one.

For all 24 h sucrose-odour memory, a single training session of sucrose paired with an odour for 2 min was employed. Blockade of the output of neurons by shi^{ts1} during the training phase, flies were placed at 32 °C 2.5 h prior to training. Manipulation of the activity of target neurons during memory consolidation phase included: 1) activation for 1 h by dTrpA1 at 30 □; and 2) blockade for 2.5 h by shi^{ts1} at 32 °C.

A performance Index (PI) was calculated by the difference between flies chose the odour paired with an unconditioned stimulus (US: high temperature or sucrose) and flies chose the other odour without US, divided by the total number of flies. A learning index (LI) was then calculated as the averaged two PIs from two reciprocal groups multiplied by 100. Half of LIs were from the first odour paired with US, and the other half of LIs from the second odour paired with US to minimize the bias of the conditioning order.

Sleep assays

Regular sleep tubes contained food of 2% agar with 5% sucrose, and the starvation sleep tubes contained only 2% agar. A female fly was anesthetized with CO_2, and then loaded into a 65 mm × 5 mm glass tube which was then placed into a *Drosophila* Activity Monitoring (DAM2, Trikinetics, Waltham) board. DAM boards were then loaded into an incubator with a 12 h:12 h light-dark cycle at 60% relative humidity, and connected to DAM system. After 2 days of entrainment, flies were recorded for another 2 days for sleep analysis. Starvation time of each genotype was consistent as in the memory tests. Flies were transferred to starvation sleep tubes between Zeitgeber Time (ZT) 23 and ZT2. The environment temperature was increased to 30 □ for 1 h to activate the neurons expressing dTrpA1, or to 32 □ for 2.5 h to inactivate the neurons expressing shi^{ts1} at ZT5/7, and then shifted the temperature back to 23 □ for another 24 h. Sleep parameters including total sleep, number of sleep episodes, and P(wake) were analyzed in 1 h bin. Sleep files acquired from DAM system were processed with DAMFileScan113X (TriKinetics Inc, Waltham, MA), and SCAMP 2019v2 using MATLAB_R2021b (MathWorks, Natick, MA). The probability of transition from a sleep to an awake state P(wake) was analyzed as previously described (Wiggin et al., 2020). The MATLAB scripts for analysis is accessed in GitHub at https://github.com/Griffith-Lab/fLy_Sleep_Probability.

For sleep with an application of gaboxadol hydrochloride (known as THIP, Cat# 85118-33-8, Sigma-Aldrich), flies were activated for 1 h at ZT7 in 2% agar starvation

tubes, and then transferred to sleep tubes containing THIP (0.1mg/ml) in 2% agar at ZT12 for 20 h.

Immunohistochemistry

Both male and female flies aged 5-7 days were used for immunostaining. Fly brains were dissected in Schneider's Drosophila Medium (1×) (Cat# 21720-024, Gibco). Dissected brains were fixed in 4% paraformaldehyde (PFA, Cat# 50-00-0, GHTECH) for 20 min at room temperature, and then washed in 1× phosphate buffered saline (PBS) containing 0.5% Triton X-100 (PBS-T) at 4 □ for 10 min for 3 times. After that, the brains were incubated in primary antibodies with 5% normal goat serum (Cat# 0005-000-121, Jackson) at 4 □ overnight. Primary antibodies used for visualization of GFP and RFP (including restricted *trans*-Tango) were: chicken anti-GFP (1:200, Cat# 13970, Abcam) and rabbit anti-DsRed (1:200, Cat# 632496, Clontech); primary antibodies used to detect GRASP signals was mouse monoclonal anti-GFP (1:200, Cat# 11814460001, Roche Applied Science). Samples were then washed in PBS-T at 4 □ for 10 min for 3 times, incubated in secondary antibodies at 4 □ overnight. Secondary antibodies (1:200) included: Alexa Fluor 488 (goat anti-chicken, Cat# A11039, Invitrogen), Alexa 568 (goat anti-rabbit, Cat# A11011, Invitrogen), Alexa Fluor 633 (goat anti-mouse, Cat# A-21052, Invitrogen). Samples were washed in PBS-T at 4 □ for 10 min for 3 times, and mounted with Vectashield (Cat# H-1000, VECTOR). Images were acquired with a Zeiss LSM 900 confocal microscope with

40× oil objective. Confocal Z-stacks were acquired in 2 μm, and analyzed using a free and open source FIJI (https://fiji.sc).

Memory phases correlated neural activity measurements

Female flies of genotypes *R58E02-p65.AD/UAS-CRTC::GFP;R37E10-GAL4.DBD /UAS-mCD8::mCherry and UAS-CRTC::GFP/+;VT064246-GAL4/UAS-mCD8:: mCherry* were employed for understanding the changes in neural activity of PAM-α1 and DPM neurons right after memory formation and after 1 h of memory consolidation. Flies were starved 26 hours when their death rate was around 10%-20% as in memory assay, and experienced different conditions at 23□：1) Trained group: a single session training of 2 min pairing of odour (CS) and sucrose (US) paradigm, 2) Un-trained group: no exposure to odour and sucrose. After training, heads were removed from the flies and sampled right after conditioning or 1 h after conditioning. Heads were fixed in 4% PFA at room temperature for 30 min, and brains were dissected for staining.

Primary antibodies used for visualization of CRTC::GFP and mCD8::mCherry were chicken anti-GFP (1:200, Cat# 13970, Abcam) and rabbit anti-DsRed (1:200, Cat# 632496, Clontech), respectively. Secondary antibodies were Alexa Fluor 488 (goat anti-chicken, Cat# A11039, Invitrogen) and Alexa 568 (goat anti-rabbit, Cat# A11011, Invitrogen).

The fluorescence level of CRTC::GFP were analyzed using Fiji. Images of cell bodies used for quantification of CRTC::GFP signals were all acquired as 8-bit

images of 1-μm-interval z-stack slices from the anterior-to-posterior, and set to the same offset for comparisons. Boundaries of cytoplasm and nuclear of a cell body were manually outlined according to mCD8::mCherry signal. Changes in CRTC::GFP nuclear signals (nuclear localization index, NLI) of each neuron was calculated using the formula as previously described (Bonheur et al., 2023): NLI = (mean nuclear GFP signal − mean cytoplasmic GFP signal) / (mean nuclear GFP signal + mean cytoplasmic GFP signal).

In vitro calcium imaging

Functional imaging experiments of neurons were performed on both male and female flies aged 5-7 days. Adult hemolymph-like saline (AHL) composed with (Concentration, mM): NaCl 108; KCl 5; NaH_2PO4 1; $MgCl_2.6H_2O$ 8.2; $CaCl_2.2H_2O$ 2; $NaHCO_3$ 4; trehalose 5; sucrose 10; and HEPES 5. Adenosine 5′-triphosphate magnesium salt (ATP, Cat# A100885, Aladdin) was dissolved in AHL immediately prior to the experiment to the final concentration of 2.5 mM. Tetrodotoxin (TTX, Cat# 554412, Sigma-Aldrich) and dopamine (DA, Cat# 73483, Sigma-Aldrich) were made freshly to final concentrations of 1 μM and 1 mM, respectively.

Flies of genotypes *w^{1118};R58E02-LexA/+;VT064246-GAL4/LexAop-P2X_2,UAS-GCaMP6f,* *w^{1118};UAS-dcr2/+;VT046004-GAL4/UAS-EPAC,* *w^{1118};UAS-dcr2/UAS-Dop1R1.RNAi;VT046004-GAL4/UAS-EPAC,* *w^{1118};UAS-dcr2/UAS-Dop1R2.RNAi;VT*

046004-GAL4/UAS-EPAC, w^{1118};UAS-dcr2/UAS-DopEcR.RNAi;VT046004-GAL4/ UAS-EPAC and *w^{1118};UAS-P2X$_2$,LexAop-GCaMP6f/R58E02-p65.AD;VT064246-LexA /R37E10-GAL4.DBD* were employed. Flies were anesthetized on ice, and brains were dissected in AHL (PH = 7.5) at room temperature. Dissected brains were then pinned to a layer of Sylgard silicone (Dow Corning, Midland, MI) in a perfusion chamber containing AHL. Drugs were applied though a gravity-fed ValveLink perfusion system that allowed a switch from one channel to the other (Automate Scientific, Berkeley, CA).

For functional connectivity experiments, after 30 s of baseline recording with perfusion of AHL, ATP was delivered for 90 s. As a control condition, AHL was perfused for 30 s and switched to a second channel of AHL for another 90 s. Brains expressing the GCaMP6f were imaged using an Mshot MF43-N fluorescence microscope (Mshot, Guangdong, China) under an Olympus × 40 (0.80W, LUMPlanFL N) water-immersion objective, and recordings were captured using a camera of Hamamatsu ORCA-Flash4.0 LT+. Images were captured using hCimage Live software. Regions of interests (ROIs) were selected in the MB of PAM/PAM-α1 and cell bodies of DPM neurons. ROIs were analyzed using FIJI. The percent change in fluorescence over time was calculated using $\Delta F / F = (F_n - F_0) / F_0 \times 100\%$ as we previously described (Liu et al., 2019). F_n is the fluorescence at time point n, and F_0 is

the fluorescence at time 0. Averaged fluorescence change values were quantified for periods of 0-30 s and 31-120 s, respectively.

For EPAC experiments, brains were exposed to fluorescent light for 5 min to reduce the photobleaching rates between the CFP and YPF. Also, TTX was applied for 5 min prior to the recording to block voltage-dependent sodium channels and throughout the entire recording period. After 30 s of baseline recording, DA was delivered for 120 s and switched back to TTX again for another 30 s. Brains expressing the FRET sensor EPACcamps1 were imaged using an Olympus BX51WI fluorescence microscope (Olympus, Center Valley, PA) under an Olympus ×40 (0.8W, LUMPlanFI) water-immersion objective, and recordings were captured using a charge-coupled device camera (Hamamatsu ORCAC472-80-12AG). Images were captured using μManager acquisition software (Edelstein et al., 2010). ROIs analysis was the same as previously described using custom software developed in MATLAB (Liu et al., 2019). Identical ROIs were selected from both the CFP and YFP channels, and calculated the ratio of normalized CFP/YFP to the first 20 frames of baseline recording for each time point. The maximum change values were determined for each group during drug perfusion period (31-150 s) and TTX washout period (151-240 s) for the following quantification.

Experimental design and statistical analysis

All the raw data were analyzed using the Prism 9.0 software (GraphPad). For most memory experiments, datasets with normal distribution, a one-way ANOVA followed by Sidak's multiple comparisons test was applied. For those did not have a normal distribution, nonparametric statistics, Kruskal-Wallis, followed by Dunn's multiple comparisons test was applied. For induced appetitive memory experiment (Figure 3A), *in vitro* functional imaging experiments (Figures 2A, B and 9B) and immunostained CRTC::GFP experiments (Figure 9D, E), two-way ANOVA followed by Dunnett's multiple comparisons test was applied. Furthermore, in the experiments to compare the activation group to the no-activation group (Figure 6F), an unpaired t test or nonparametric test was applied based on data distribution. For sleep experiments, a two-way ANOVA followed by Dunn's multiple comparisons test was applied to determine statistical significance between the experimental groups and the control groups for each 1 h bin. All data were presented as mean ± standard error (SEM). A statistically significant difference was set to $p < 0.05$. Detailed statistical analysis of each experiment was summarized in Tables 1-4: Table 1 for one-way ANOVA analysis, Table 2 for unpaired t-test analysis, Table 4 for two-way ANOVA analysis for sleep, and Table 3 for the rest two-way ANOVA analysis.

Additional information

Conflict of Interest: The authors declare no competing interests.

Acknowledgments: This work is supported by National Natural Science Foundation of China (32071009, 32371063, 82341248 to C.L.), Guangdong Basic and Applied Basic Research Foundation (2024A151501150 to C.L.), CAS Key Laboratory of Brain Connectome and Manipulation (2019DP173024) and National Institute of Health grant R01MH67284 (to L.C.G.). We thank Kristine Paik for help with the behavioral experiments at the beginning of this study, Dr. Martha L. Reed and all lab members for their valuable discussion.

Author Contributions

C.L. designed and supervised research; L.Y., L.W., T.D.W., X.S., W.Y., H.L., and C.L. performed research; L.Y., L.L., Z.L., Y.L., Z.M., F.G., L.C.G. and C.L. analyzed and interpreted data; L.Y., F.L., L.C.G. and C.L. wrote the manuscript and all authors reviewed the manuscript.

Data availability statement

All data are contained within the manuscript. Statistical analysis details, including sample size, statistical tests and p values have been provided in Tables 1-4. This work generated fly stocks, which we will distribute on request. Raw data will be distributed on request.

Declaration of interests

Authors declare that they have no conflict of interest.

References

Adel MG, L. C. 2021. The Role of Dopamine in Associative Learning in Drosophila An Updated Unified Model. Neurosci Bull 37:831-852. DOI: 10.1007/s12264-021-00665-0, PMID: 33779893

Aso Y, Rubin GM. 2016. Dopaminergic neurons write and update memories with cell-type-specific rules. Elife 5. DOI: 10.7554/eLife.16135, PMID: 27441388

Aso Y, Rubin GM. 2020. Toward nanoscale localization of memory engrams in Drosophila. J Neurogenet 34:151-155. DOI:10.1080/01677063.2020.1715973, PMID: 31985306

Aso Y, Herb A, Ogueta M, Siwanowicz I, Templier T, Friedrich AB, Ito K, Scholz H, Tanimoto H. 2012. Three dopamine pathways induce aversive odor memories with different stability. pLoS Genet 8:e1002768. DOI: 10.1371/journal.pgen.1002768, PMID: 22807684

Aso Y, Hattori D, Yu Y, Johnston RM, Iyer NA, Ngo TT, Dionne H, Abbott LF, Axel R, Tanimoto H, Rubin GM. 2014a. The neuronal architecture of the mushroom body provides a logic for associative learning. Elife 3:e04577. DOI: 10.7554/eLife.04577, PMID: 25535793

Aso Y, D Sitaraman, T Ichinose, KR Kaun, K Vogt, G Belliart-Guerin, PY Placais, AA Robie, N Yamagata, C Schnaitmann, WJ Rowell, RM Johnston, TT Ngo, N Chen, W Korff, MN Nitabach, U Heberlein, T Preat, KM Branson, H Tanimoto and GM Rubin. 2014b. Mushroom body output neurons encode valence and guide memory-based action selection in Drosophila. Elife 3:e04580. DOI:10.7554/eLife.04580, PMID: 25535794

Berry JA, Cervantes-Sandoval I, Nicholas EP, Davis RL. 2012. Dopamine is required for learning and forgetting in Drosophila. Neuron 74:530-542. DOI: 10.1016/j.neuron.2012.04.007, PMID: 22578504

Berry JA, Cervantes-Sandoval I, Chakraborty M, Davis RL. 2015. Sleep Facilitates Memory by Blocking Dopamine Neuron-Mediated Forgetting. Cell 161:1656-1667. DOI: 10.1016/j.cell.2015.05.027, PMID: 26073942

Bonheur M, Swartz KJ, Metcalf MG, Wen X, Zhukovskaya A, Mehta A, Connors KE, Barasch JG, Jamieson AR, Martin KC, Axel R, Hattori D. 2023. A rapid and bidirectional reporter of neural activity reveals neural correlates of social behaviors in Drosophila. Nat Neurosci 26:1295-1307. DOI: 10.1038/s41593-023-01357-w, PMID: 37308660

Brodt S, Inostroza M, Niethard N, Born J. 2023. Sleep-A brain-state serving systems memory consolidation. Neuron 111:1050-1075. DOI: 10.1016/j.neuron.2023.03.005, PMID: 37023710

Burke CJ, Huetteroth W, Owald D, Perisse E, Krashes MJ, Das G, Gohl D, Silies M, Certel S, Waddell S. 2012. Layered reward signalling through octopamine and dopamine in Drosophila. Nature 492:433-437. DOI: 10.1038/nature11614, PMID: 23103875

Cervantes-Sandoval I, Davis RL (2012) Distinct traces for appetitive versus aversive olfactory memories in DPM neurons of Drosophila. Curr Biol 22:1247-1252. DOI: 10.1016/j.cub.2012.05.009, PMID: 22658595

Chandra R, F Farah, F Munoz-Lobato, A Bokka, KL Benedetti, C Brueggemann, MFA Saifuddin, JM Miller, J Li, E Chang, A Varshney, V Jimenez, A Baradwaj, C Nassif, S Alladin, K Andersen, AJ Garcia, V Bi, SK Nordquist, RL Dunn, V Garcia, K Tokalenko, E Soohoo, F Briseno, S Kaur, M Harris, H Guillen, D Byrd, B Fung, AE Bykov, E Odisho, B Tsujimoto, A Tran, A Duong, KC Daigle, R Paisner, CE Zuazo, C Lin, A Asundi, MA Churgin, C Fang-Yen, M Bremer, S Kato, MK VanHoven and ND L'Etoile. 2023. Sleep is required to consolidate odor memory and remodel olfactory synapses. Cell 186:2911-2928. DOI: 10.1016/j.cell.2023.05.006, PMID: 37269832

Chouhan NS, Griffith LC, Haynes P, Sehgal A. 2021. Availability of food determines the need for sleep in memory consolidation. Nature 589:582-585. DOI: 10.1038/s41586-020-2997-y, PMID: 33268891

Chouhan NS, Sehgal A. 2022. Consolidation of Sleep-Dependent Appetitive Memory Is Mediated by a Sweet-Sensing Circuit. J Neurosci 42:3856-3867. DOI: 10.1523/JNEUROSCI.0106-22.2022, PMID: 35361706

Dag U, Lei Z, Le JQ, Wong A, Bushey D, Keleman K. 2019. Neuronal reactivation during post-learning sleep consolidates long-term memory in Drosophila. Elife 8. DOI: 10.7554/eLife.42786, PMID: 30801246

Diekelmann S, Born J. 2010. The memory function of sleep. Nat Rev Neurosci 11:114-126. DOI: 10.1038/nrn2762, PMID: 20046194

Dissel S, Angadi V, Kirszenblat L, Suzuki Y, Donlea J, Klose M, Koch Z, English D, Winsky-Sommerer R, van Swinderen B, Shaw PJ. 2015. Sleep restores behavioral plasticity to Drosophila mutants. Curr Biol 25:1270-1281. DOI: 10.1016/j.cub.2015.03.027, PMID: 25913403

Donlea JMT, M.S. Suzuki, Y. Gottschalk, L. Shaw, P.J. 2011. Inducing Sleep by Remote Control Facilitates Memory Consolidation in Drosophila. Science 332:1571-1576. DOI: 10.1126/science.1202249, PMID: 21700877

Driscoll M, Buchert SN, Coleman V, McLaughlin M, Nguyen A, Sitaraman D. 2021. Compartment specific regulation of sleep by mushroom body requires GABA and dopaminergic signaling. Sci Rep 11:20067. DOI: 10.1038/s41598-021-99531-2, PMID: 34625611

Dubnau J, Chiang AS. 2013. Systems memory consolidation in Drosophila. Curr Opin Neurobiol 23:84-91. DOI: 10.1016/j.conb.2012.09.006.

Dudai Y, Karni A, Born J. 2015. The Consolidation and Transformation of Memory. Neuron 88:20-32. DOI: 10.1016/j.neuron.2015.09.004, PMID: 26447570

Edelstein A, Amodaj N, Hoover K, Vale R, Stuurman N. 2010. Computer control of microscopes using microManager. Curr Protoc Mol Biol Chapter 14:Unit14 20. DOI: 10.1002/0471142727.mb1420s92, PMID: 20890901

Feinberg EH, Vanhoven MK, Bendesky A, Wang G, Fetter RD, Shen K, Bargmann CI. 2008. GFP Reconstitution Across Synaptic Partners (GRASP) defines cell contacts and synapses in living nervous systems. Neuron 57:353-363. DOI: 10.1016/j.neuron.2007.11.030, PMID: 18255029

Feng KL, Weng JY, Chen CC, Abubaker MB, Lin HW, Charng CC, Lo CC, de Belle JS, Tully T, Lien CC, Chiang AS. 2021. Neuropeptide F inhibits dopamine neuron interference of long-term memory consolidation in Drosophila. iScience 24:103506. DOI: 10.1016/j.isci.2021.103506, PMID: 34934925

Girardeau G, Lopes-Dos-Santos V. 2021. Brain neural patterns and the memory function of sleep. Science 374:560-564. DOI: 10.1126/science.abi8370, PMID: 34709916

Hamada FN, Rosenzweig M, Kang K, Pulver SR, Ghezzi A, Jegla TJ, Garrity PA. 2008. An internal thermal sensor controlling temperature preference in Drosophila. Nature 454:217-220. DOI: 10.1038/nature07001, PMID: 18548007

Haynes PR, Christmann BL, Griffith LC. 2015. A single pair of neurons links sleep to memory consolidation in Drosophila melanogaster. Elife 4. DOI: 10.7554/eLife.03868, PMID: 25564731

Huang C, Zheng X, Zhao H, Li M, Wang P, Xie Z, Wang L, Zhong Y. 2012. A permissive role of mushroom body alpha/beta core neurons in long-term memory consolidation in Drosophila. Curr Biol 22:1981-1989. DOI: 10.1016/j.cub.2012.08.048, PMID: 23063437

Huetteroth W, Perisse E, Lin S, Klappenbach M, Burke C, Waddell S. 2015. Sweet taste and nutrient value subdivide rewarding dopaminergic neurons in Drosophila. Curr Biol 25:751-758. DOI: 10.1016/j.cub.2015.01.036, PMID: 25728694

Ichinose T, Aso Y, Yamagata N, Abe A, Rubin GM, Tanimoto H. 2015. Reward signal in a recurrent circuit drives appetitive long-term memory formation. Elife 4:e10719. DOI: 10.7554/eLife.10719, PMID: 26573957

Jovanoski KD, Duquenoy L, Mitchell J, Kapoor I, Treiber CD, Croset V, Dempsey G, Parepalli S, Cognigni P, Otto N, Felsenberg J, Waddell S. 2023. Dopaminergic systems create reward seeking despite adverse consequences. Nature 623:356-365. DOI: 10.1038/s41586-023-06671-8, PMID: 37880370

Keene AC, Krashes MJ, Leung B, Bernard JA, Waddell S. 2006. Drosophila dorsal paired medial neurons provide a general mechanism for memory consolidation. Curr Biol 16:1524-1530. DOI: 10.1016/j.cub.2006.06.022.

Keene AC, Stratmann M, Keller A, Perrat PN, Vosshall LB, Waddell S. 2004. Diverse odor-conditioned memories require uniquely timed dorsal paired medial neuron output. Neuron 44:521-533. DOI: 10.1016/j.neuron.2004.10.006, PMID: 15504331

Keene AC, Duboue ER, McDonald DM, Dus M, Suh GS, Waddell S, Blau J. 2010. Clock and cycle limit starvation-induced sleep loss in Drosophila. Curr Biol 20:1209-1215. DOI: 10.1016/j.cub.2010.05.029, PMID: 20541409

Kim YC, Lee HG, Han KA. 2007. D1 dopamine receptor dDA1 is required in the mushroom body neurons for aversive and appetitive learning in Drosophila. J Neurosci 27:7640-7647. DOI: 10.1523/JNEUROSCI.1167-07.2007, PMID: 17634358

Kjaerby C, Andersen M, Hauglund N, Untiet V, Dall C, Sigurdsson B, Ding F, Feng J, Li Y, Weikop P, Hirase H, Nedergaard M. 2022. Memory-enhancing properties of sleep depend on the oscillatory amplitude of norepinephrine. Nat Neurosci 25:1059-1070. DOI: 10.1038/s41593-022-01102-9, PMID: 35798980

Klinzing JG, Niethard N, Born J. 2019. Mechanisms of systems memory consolidation during sleep. Nat Neurosci 22:1598-1610. DOI: 10.1038/s41593-019-0467-3, PMID: 31451802

Krashes MJ, Waddell S. 2008. Rapid consolidation to a radish and protein synthesis-dependent long-term memory after single-session appetitive olfactory conditioning in Drosophila. J Neurosci 28:3103-3113. DOI: 10.1523/JNEUROSCI.5333-07.2008, PMID: 18354013

Krashes MJ, Keene Ac Fau- Leung B, Leung B Fau- Armstrong JD, Armstrong Jd Fau- Waddell S, Waddell S. 2007. Sequential use of mushroom body neuron subsets during drosophila odor memory processing. Neuron 53:103-115. DOI: 10.1016/j.neuron.2006.11.021, PMID: 17196534

Krashes MJ, DasGupta S, Vreede A, White B, Armstrong JD, Waddell S. 2009. A neural circuit mechanism integrating motivational state with memory expression in Drosophila. Cell 139:416-427. DOI: 10.1016/j.cell.2009.08.035, PMID: 19837040

Krishnan HC, Gandour CE, Ramos JL, Wrinkle MC, Sanchez-Pacheco JJ, Lyons LC. 2016. Acute Sleep Deprivation Blocks Short- and Long-Term Operant Memory in Aplysia. Sleep 39:2161-2171. DOI: 10.5665/sleep.6320, PMID: 27748243

Kruttner S, Traunmuller L, Dag U, Jandrasits K, Stepien B, Iyer N, Fradkin LG, Noordermeer JN, Mensh BD, Keleman K. 2015. Synaptic Orb2A Bridges Memory Acquisition and Late Memory Consolidation in Drosophila. Cell Rep 11:1953-1965. DOI: 10.1016/j.celrep.2015.05.037, PMID: 26095367

Kume K, Kume S, Park SK, Hirsh J, Jackson FR. 2005. Dopamine is a regulator of arousal in the fruit fly. J Neurosci 25:7377-7384. DOI: 10.1523/JNEUROSCI.2048-05.2005, PMID: 26095367

Li X, F Yu and A Guo. 2009. Sleep deprivation specifically impairs short-term olfactory memory in Drosophila. Sleep 32:1417-24. DOI:10.1093/sleep/32.11.1417, PMID: 19928381

Lin S, B Senapati and CH Tsao. 2019. Neural basis of hunger-driven behaviour in Drosophila. Open Biol 9:180259. DOI: 10.1098/rsob.180259, PMID: 30914005

Lipinska G and KGF Thomas. 2019. The Interaction of REM Fragmentation and Night-Time Arousal Modulates Sleep-Dependent Emotional Memory Consolidation. Front Psychol 10:1766. DOI: 10.3389/fpsyg.2019.01766, PMID: 31428021

Liu C, Z Meng, TD Wiggin, J Yu, ML Reed, F Guo, Y Zhang, M Rosbash and LC Griffith. 2019. A Serotonin-Modulated Circuit Controls Sleep Architecture to Regulate Cognitive Function Independent of Total Sleep in Drosophila. Curr Biol 29:3635-3646 e5. DOI: 10.1016/j.cub.2019.08.079, PMID: 31668619

Liu C, PY Placais, N Yamagata, BD Pfeiffer, Y Aso, AB Friedrich, I Siwanowicz, GM Rubin, T Preat and H Tanimoto. 2012. A subset of dopamine neurons signals reward for odour memory in Drosophila. Nature 488:512-6. DOI: 10.1038/nature11304, PMID: 22810589

Liu Q, M Tabuchi, S Liu, L Kodama, W Horiuchi, J Daniels, L Chiu, D Baldoni and MN Wu. 2017. Branch-specific plasticity of a bifunctional dopamine circuit encodes protein hunger. Science 356:534-539. DOI: 10.1126/science.aal3245, PMID: 28473588

MacFadyen UMO, I. Lewis, S.A. 1973. Starvation and human slow-wave sleep. J Appl Physiol, 35:391-394.

Macpherson LJ, EE Zaharieva, PJ Kearney, MH Alpert, TY Lin, Z Turan, CH Lee and M Gallio. 2015. Dynamic labelling of neural connections in multiple colours by trans-synaptic fluorescence complementation. Nat Commun 6:10024. DOI: 10.1038/ncomms10024, PMID: 26635273

Manassero E, A Giordano, E Raimondo, A Cicolin and B Sacchetti. 2022. Sleep Deprivation During Memory Consolidation, but Not Before Memory Retrieval, Widens Threat Generalization to New Stimuli. Front Neurosci 16:902925. DOI: 10.3389/fnins.2022.902925.

Mao Z and RL Davis. 2009. Eight different types of dopaminergic neurons innervate the Drosophila mushroom body neuropil: anatomical and physiological heterogeneity. Front Neural Circuits 3:5. DOI: 10.3389/neuro.04.005.2009, PMID: 19597562

McDonald DM, and Keene, A.C. 2010. The sleep feeding conflict: Understanding behavioral integration through genetic analysis in Drosophila. Aging (Albany NY) 2:519-522. DOI: 10.18632/aging.100181, PMID: 20689154

McGaugh J. 2000. Memory--a century of consolidation. Science (New York, N.Y.) 287:248-51. DOI: 10.1126/science.287.5451.248, PMID: 10634773

Melnattur K and P Shaw. 2019. Staying awake to stay alive: A circuit controlling starvation-induced waking. PLoS Biol 17:e3000199. DOI: 10.1371/journal.pbio.3000199, PMID: 30917116

Okray Z, Jacob PF, Stern C, Desmond K, Otto N, Talbot CB, Vargas-Gutierrez P, Waddell S. 2023. Multisensory learning binds neurons into a cross-modal memory engram. Nature 617:777-784. DOI: 10.1038/s41586-023-06013-8, PMID: 37100911

Pavlov IP. 1927. Conditioned reflexes: an investigation of the physiological activity of the cerebral cortex. Oxford University Press.

Placais PY, S Trannoy, G Isabel, Y Aso, I Siwanowicz, G Belliart-Guerin, P Vernier, S Birman, H Tanimoto and T Preat. 2012. Slow oscillations in two pairs of

dopaminergic neurons gate long-term memory formation in Drosophila. Nat Neurosci 15:592-9. DOI: 10.1038/nn.3055, PMID: 22366756

Plaza SM, J Clements, T Dolafi, L Umayam, NN Neubarth, LK Scheffer and S Berg. 2022. neuPrint: An open access tool for EM connectomics. Front Neuroinform 16:896292. DOI: 10.3389/fninf.2022.896292, PMID: 35935535

Qin H, M Cressy, W Li, JS Coravos, SA Izzi and J Dubnau. 2012. Gamma neurons mediate dopaminergic input during aversive olfactory memory formation in Drosophila. Curr Biol 22:608-14. DOI: 10.1016/j.cub.2012.02.014, PMID: 22425153

Quinn WGH, W.A. Benzer, S. 1974. Conditioned Behavior in Drosophila melanogaster. Proc Nat Acad Sci USA 71:708-712. DOI: 10.1073/pnas.71.3.708, PMID: 4207071

Roesler R, McGaugh JL. 2010. Memory Consolidation. In: Encyclopedia of Behavioral Neuroscience (Koob GF, Moal ML, Thompson RF, eds), pp 206-214. Oxford: Academic Press.

Rolls A, Colas D, Adamantidis A, Carter M, Lanre-Amos T, Heller HC, de Lecea L. 2011. Optogenetic disruption of sleep continuity impairs memory consolidation. Proc Natl Acad Sci U S A 108:13305-13310. DOI: 10.1073/pnas.1015633108, PMID: 21788501

Sabandal JM, Berry JA, Davis RL. 2021. Dopamine-based mechanism for transient forgetting. Nature 591:426-430. DOI: 10.1038/s41586-020-03154-y, PMID: 33473212

Scheffer LK, CS Xu, M Januszewski, Z Lu, SY Takemura, KJ Hayworth, GB Huang, K Shinomiya, J Maitlin-Shepard, S Berg, J Clements, PM Hubbard, WT Katz, L Umayam, T Zhao, D Ackerman, T Blakely, J Bogovic, T Dolafi, D Kainmueller, et al. 2020. A connectome and analysis of the adult Drosophila central brain. Elife 9. DOI: 10.7554/eLife.57443, PMID: 32880371

Senapati B, Tsao CH, Juan YA, Chiu TH, Wu CL, Waddell S, Lin S. 2019. A neural mechanism for deprivation state-specific expression of relevant memories in Drosophila. Nat Neurosci 22:2029-2039. DOI: 10.1038/s41593-019-0515-z, PMID: 31659341

Sitaraman D, Y Aso, GM Rubin and MN Nitabach. 2015. Control of Sleep by Dopaminergic Inputs to the Drosophila Mushroom Body. Front Neural Circuits 9:73. DOI: 10.3389/fncir.2015.00073, PMID: 26617493

Spira AP, LP Chen-Edinboro, MN Wu and K Yaffe. 2014. Impact of sleep on the risk of cognitive decline and dementia. Curr Opin Psychiatry 27:478-83. DOI: 10.1097/YCO.0000000000000106, PMID: 25188896

Sun L, RH Jiang, WJ Ye, M Rosbash and F Guo. 2022. Recurrent circadian circuitry regulates central brain activity to maintain sleep. Neuron 110:2139-2154 e5. DOI: 10.1016/j.neuron.2022.04.010, PMID: 35525241

Tempel BLB, N.; Dawson, D.R.; Quinn, W.G. 1983. Reward learning in normal and mutant Drosophila. Proc Natl Acad Sci U S A 80:1482-1486. DOI: 10.1073/pnas.80.5.1482, PMID: 6572401

Thimgan MS, Suzuki Y, Seugnet L, Gottschalk L, Shaw PJ. 2010 The perilipin homologue, lipid storage droplet 2, regulates sleep homeostasis and prevents learning impairments following sleep loss. PLoS Biol. 8(8). DOI: 10.1371/journal.pbio.1000466, PMID: 20824166

Tomita J, G Ban, YS Kato and K Kume. 2021. Protocerebral Bridge Neurons That Regulate Sleep in Drosophila melanogaster. Front Neurosci 15:647117. DOI: 10.3389/fnins.2021.647117, PMID: 34720844

Tonegawa S, MD Morrissey and T Kitamura. 2018. The role of engram cells in the systems consolidation of memory. Nat Rev Neurosci 19:485-498. DOI: 10.1038/s41583-018-0031-2, PMID: 29970909

Tsao CH, CC Chen, CH Lin, HY Yang and S Lin. 2018. Drosophila mushroom bodies integrate hunger and satiety signals to control innate food-seeking behavior. Elife 7. 10.7554/eLife.35264, PMID: 29547121

Tully TQ, W.G. 1985. Classical conditioning and retention in normal and mutant Drosophila melanogaster. J Comp Physiol A 157:263-277. DOI: 10.1007/BF01350033, PMID: 3939242

Ueno T, J Tomita, H Tanimoto, K Endo, K Ito, S Kume and K Kume. 2012. Identification of a dopamine pathway that regulates sleep and arousal in Drosophila. Nat Neurosci 15:1516-23. DOI: 10.1038/nn.3238.

Van Swinderen B and R Andretic. 2011. Dopamine in Drosophila: setting arousal thresholds in a miniature brain. Proc Biol Sci 278:906-13. DOI: 10.1098/rspb.2010.2564, PMID: 21208962

Waddell SA, J.D.; Kitamoto, T.; Kaiser, K.; Quinn, W.G. 2000. The amnesiac gene product is expressed in two neurons in the Drosophila brain that are critical for memory. cell 103:803-815. DOI: 10.1016/s0092-8674(00)00183-5, PMID: 11114336

Wiggin TD, Goodwin PR, Donelson NC, Liu C, Trinh K, Sanyal S, Griffith LC. 2020. Covert sleep-related biological processes are revealed by probabilistic analysis in Drosophila. Proc Natl Acad Sci U S A 117:10024-10034. DOI: 10.1073/pnas.1917573117, PMID: 32303656

Yamagata N, Hiroi M, Kondo S, Abe A, Tanimoto H. 2016. Suppression of Dopamine Neurons Mediates Reward. pLoS Biol 14:e1002586. DOI: 10.1371/journal.pbio.1002586, PMID: 27997541

Yamagata N, Ezaki T, Takahashi T, Wu H, Tanimoto H. 2021. Presynaptic inhibition of dopamine neurons controls optimistic bias. Elife 10. DOI: 10. 10.7554/eLife.64907, PMID: 34061730

Yamagata N, Ichinose T, Aso Y, Placais PY, Friedrich AB, Sima RJ, Preat T, Rubin GM, Tanimoto H. 2015. Distinct dopamine neurons mediate reward signals for

short- and long-term memories. Proc Natl Acad Sci U S A 112:578-583. DOI: 10.1073/pnas.1421930112, PMID: 25548178

Yu D, Keene AC, Srivatsan A, Waddell S, Davis RL. 2005. Drosophila DPM neurons form a delayed and branch-specific memory trace after olfactory classical conditioning. Cell 123:945-957. DOI: 10.1016/j.cell.2005.09.037, PMID: 16325586

Yurgel ME, Kakad P, Zandawala M, Nassel DR, Godenschwege TA, Keene AC. 2019. A single pair of leucokinin neurons are modulated by feeding state and regulate sleep-metabolism interactions. pLoS Biol 17:e2006409. DOI: 10.1371/journal.pbio.2006409, PMID: 30759083

Zeng J, Li X, Zhang R, Lv M, Wang Y, Tan K, Xia X, Wan J, Jing M, Zhang X, Li Y, Yang Y, Wang L, Chu J, Li Y, Li Y. 2023. Local 5-HT signaling bi-directionally regulates the coincidence time window for associative learning. Neuron 111:1118-1135. DOI: 10.1016/j.neuron.2022.12.034, PMID: 3670675

Zhang X, Ren Q, Guo A. 2013. Parallel pathways for cross-modal memory retrieval in Drosophila. J Neurosci 33:8784-8793. DOI: 10.1523/JNEUROSCI.4631-12.2013, PMID: 23678121

Zheng Z, JS Lauritzen, E Perlman, CG Robinson, M Nichols, D Milkie, O Torrens, J Price, CB Fisher, N Sharifi, SA Calle-Schuler, L Kmecova, IJ Ali, B Karsh, ET Trautman, JA Bogovic, P Hanslovsky, G Jefferis, M Kazhdan, K Khairy, et al. 2018. A Complete Electron Microscopy Volume of the Brain of Adult Drosophila melanogaster. Cell 174:730-743. DOI: 10.1016/j.cell.2018.06.019, PMID: 3003336

Figure legends

Figure 1. PAM neurons form functional synapses with DPM neurons.

(A) The schematic and expression patterns of PAM and DPM neurons. PAM neurons labeled by R58E02-LexA are visualized by GFP (green), and DPM neurons labeled by eyeless-GAL80;MB-GAL80;c316-GAL4 are visualized by RFP (magenta). (B) Fragment of spGFP1-10 and nSyb-GFP1-10 is expressed in R58E02-GAL4 and LexA+ neurons, and fragment of spGFP11 is expressed L0111-LexA and eyeless-GAL80;MB-GAL80;c316-GAL4+ neurons, respectively. Reconstituted GFP signals are shown as puncta (green). The mushroom body is outlined with dashed lines. (C) Newly generated VT064246-LexA (II) and VT064246-LexA (III) recapitulate expression pattern of DPM neurons labeled with VT064246-GAL4. (D) Schematic of restricted *trans*-Tango for direct synaptic contacts between PAM-GAL4 (R58E02) labeled upstream neurons and DPM-LexA (VT064246) labeled targeted postsynaptic to PAM neurons. Anti-GFP-labeled neurons are the downstream of PAM neurons. Anti-RFP-labeled neurons are non-downstream neurons. Right lower panels, the control of restricted *trans*-Tango. Signals of downstream target of DPM neurons was not detected without PAM driver R58E02-GAL4. Scale bar: 20 μm.

Figure 2. PAM neurons inhibit DPM neurons via DA receptors.

(A) Functional connection between PAM neurons and DPM neurons. Averaged GCaMP traces and quantification of DPM neurons in response to activation of $P2X_2$

expressing PAM neurons by application of 2.5 mM ATP. n = 22-25. (B) Averaged cAMP traces and quantification of DPM neurons in response to DA with the presence of 2.0 mM TTX when Dop1R1, Dop1R2 and DopEcR were knocked down. n = 11 for all groups. $^{*}p<0.05$; $^{***}p<0.001$; $^{****}p<0.0001$. Curves are represented as mean for clarity. Bar graph are represented as mean ± SEM with individual values. See also Table 3.

Figure 3. Activation of PAM neurons during consolidation impairs long-term memory, possibly via inhibiting DPM neurons.

(A) Left panel: the paradigm of 1 min association of activation of neurons with odours for training. M: MCH; O: OCT. Red line: 30 □; black line: 23 □. Right panel: activation of PAM neurons pairing with an odour in non-starved and starved flies are sufficient to induce 2 min appetitive memory. n = 16 for all groups. (B) The paradigm of a single session training with 2 min association of sucrose (Green) and an odour, and the paradigm of 24 h appetitive memory with blocking the output of neurons for 2.5 h before and during training at 32 □ (left). Inactivation of PAM neurons during training impaired 24 h memory (Right). n = 8-10. (C) Schematic of innervations of DPM neurons on all lobes of MB (left). Inactivation of DPM neurons for 2.5 h after training disrupts 24 h memory (right). (D) Inactivation of DPM neurons labeled by VT064246-GAL4 after training for 2.5 h impaired 24 h memory. n = 28-30. (E) Inactivation of DPM neurons during training did not impair 24 h memory. n = 6-9. (F)

Schematic of innervations of R58E02-GAL4 labeling (PAM) neurons on the horizontal lobes of MB, including subdomains of γ1-5, β'2, β1-2 and α1 (left). Different gray scales were for each compartment's visibility, not projection intensity. Activation of PAM neurons for 1 h after training disrupts 24 h memory (right). (G) Flies form 24 h appetitive memory without activation of R58E02-GAL4+ neurons. n = 14-18. (H) Inactivation of PAM neurons after training for 2.5 h did not impair 24 h memory. n = 14-15. Red line: 30 □; blue line: 32 □. n.s.: not significant; $^{*}p<0.05$; $^{**}p<0.01$; $^{***}p<0.001$; $^{****}p<0.0001$. Bar graph are represented as mean ± SEM with individual values. See also Table 1.

Figure 4. Increased or decreased activity of PAM/DPM neurons results reduced and fragmented sleep.

(A) Timeline for sleep recording with activation of PAM neurons for 1 h before, during and after activation till supposed 24 h memory test. Total sleep (upper panel), number of sleep episodes (middle panel), and P(wake) (probability of transition from a sleep to an awake status) (lower panel) in 1 h bin for activation of PAM neurons. n = 40-43. (B) Inactivation of PAM neurons labeled by R58E02-GAL4 under starvation resulted in a significant decrease of sleep at early night, with increased number of sleep episodes and P(wake). n = 33-39. (C) Timeline for sleep recording with inactivation of DPM neurons labeled by c316-GAL4 for 2.5 h before, during and after activation till supposed 24 h memory test. Total sleep, number of sleep episodes, and

P(wake) in 1 h bin for inactivation of DPM neurons. n = 33-43. (D) Inactivation of DPM neurons labeled by VT064246-GAL4 with starvation resulted in a decreased and fragmented sleep after activation at night, but almost no effect on P(wake). n = 11-37. Red line: 30 □; blue line: 32 □; LP1: light period on day 1; red box: activation of neurons for 1 h; DP1 (grey box): dark period on day 1; LP2: light period on day 2; ZT: Zeitgeber time. See also Table 4.

Figure 5. PAM-DPM interactions in sleep regulation are likely to be context-dependent.

(A) Activation of PAM neurons without starvation resulted a reduction of sleep at early night, as well as a slight decrease in number of sleep episodes, but an increase in P(wake). n = 39-42. (B) Inactivation of PAM neurons had no effect on sleep without starvation. n = 22-27. (C) Inactivation of DPM neurons labeled by eyeless-GAL80;MB-GAL80;c316-GAL4 without starvation had barely no effects on sleep. n = 35-47. (D) Inactivation of DPM neurons labeled by VT064246-GAL4 had mild effect in sleep at early phase after inactivation without starvation. n = 27-36. Sleep data were presented in 1 h bin. White box: light period; red box: activation period; grey box, dark period; solid fill: starvation; patterned fill: no starvation. See also Table 4.

Figure 6. The PAM-α1 subset of PAM neurons contributes to memory consolidation.

(A, C) The expression pattern of LTM-PAM and STM-PAM neurons labeled by R15A04-GAL4 and R48B04-GAL4, respectively. Upper panels, cell body; middle panels, projections on the MB; lower panels, schematic of the projections on the horizontal lobes. Scale bar: 20 μm. (B, D) The paradigm of 24 h memory by activation of LTM/STM-PAM neurons for 1 h after training. Activation of R15A04-GAL4+ neurons impairs 24 h memory (B). Activation of R48B04-GAL4+ neurons has no effect on 24 h memory (D). n = 15-21. (E) The expression patterns of specific subtypes of LTM-PAM neurons labeled by split-GAL4 lines: MB299B and MB043B (α1), MB213B (β1/β2), MB025B (β'1), MB032B (β'2), MB315C (γ5). Scale bar: 20 μm. (F) Left panel, activation and no-activation of subtypes of LTM-PAM neurons. Right panel, activation of MB299B and MB043B which project to α1 subdomain impairs LTM compared to the no-activation group. n = 5-12. (G) The differences in cell number/identity between the two drivers of MB299B and MB043B. "+" with greyscales indicated the levels of projections of a driver in MB subdomains; "-" indicated no projections. See also Tables 1 and 2.

Figure 7. The PAM-α1 subset of PAM neurons contributes to linking memory consolidation and sleep.

(A) Flies with activation of MB299B-GAL4+ neurons after training for 1 h exhibited impaired 24 h memory compared to their genetic controls. n = 14-17. (B) Activation of PAM-α1 neurons labeled by MB043B after training for 1 h impaired 24 h memory. n = 16-20. (C) Flies with blockade the output of MB299B-GAL4+ neurons after training for 2.5 h exhibited an impairment of 24 h memory compared to genetic controls. n = 11-14. (D) Inactivation of PAM-α1 neurons labeled by MB043B after training for 2.5 h did not affect 24 h memory. n = 16-25. (E) 1 h activation of PAM-α1 neurons labeled by MB299B prior to and during the test impaired 24 h memory. n = 11-17. (F) Activation of PAM-α1 neurons labeled by MB299B during the test did not affect 24 h memory. n = 18-23. (G) Inhibition of PAM-α1 neurons labeled by MB299B prior to and during the test for 30 min did not affect 24 h memory. n = 9-10. (H) Upper panel: the paradigm for sleep recording under starvation. Lower panel: total sleep, number of sleep episodes, and P(wake) in 1 h bin for activation of PAM-α1 neurons labeled by MB299B. n = 22-30. (I) Inactivation of PAM-α1 neurons labeled by MB299B under starvation had no effects on sleep. n = 33-39. (J) Activation of PAM-α1 neurons labeled by MB043B for 1 h reduced total sleep, increased the number of sleep episodes and P(wake) especially during the dark period. n = 23-30. (K) Inactivation of PAM-α1 neurons labeled by MB043B under starvation significantly reduced total sleep, and increased both the number of sleep episodes and P(wake), especially during the dark period. n = 30-39. See also Tables 1 and 4.

Figure 8. The PAM-α1 subset linking memory consolidation and sleep depends on internal starvation status.

(A-B) Sleep profiles of total sleep, the number of sleep episodes, and P(wake) with 1 h activation of MB299B (A) or MB043B (B) before, during and after activation. Sleep was not affected without starvation. n = 28-31. (C) Inactivation of MB299B for 2.5 h without starvation had no effects on sleep. n = 30-37. (D) Inactivation of MB043B for 2.5 h without starvation resulted a significant reduction in total sleep, a mild increase of number of sleep episodes during the dark period, and no effect on P(wake). n = 30-39. See also Table 4.

Figure 9. A specific PAM-α1-DPM inhibitory microcircuit maintains basal activity post-learning.

(A) Characterization of anatomical connections of PAM-α1-DPM microcircuit. Left panel: 3D view of expression patterns of PAM-α1 neurons (colored) and DPM neurons (grey) from NeuPrint. Right panel: synaptic connections between 14 PAM-α1 neurons and 2 DPM neurons with their identity number based on the Hemibrain connectome dataset. (B) Activation of $P2X_2$ expressing PAM-α1 neurons labeled by MB299B by application of ATP reduced GCaMP levels in DPM neurons labeled by VT064246-LexA. n = 10-18. (C) Paradigm for appetitive olfactory training and vehicle un-trained control, and representative neural activities reflected by CRTC::GFP in cell bodies of PAM-α1 and DPM neurons at two time points post

training. mCD8::mCherry was used to demarcate nucleus and cytoplasm (white dotted circles). (D-E) Quantification of nucleus localization index (NLI) of PAM-α1 and DPM neurons under un-starved, un-trained and trained conditions at two time points. n = 19-20 of PAM-α1 neurons from 6 brains; n = 8-10 of DPM neurons from 9 brains. Scale bar: 5 μm. #: significance between fed and starved groups; *: significance between trained and un-trained groups under starvation. See also Tables 1 and 3.

Figure 10. The PAM-α1-DPM inhibitory microcircuit binds memory consolidation and sleep in an internal-state dependent manner.

(A) Simultaneous silence of PAM-α1-DPM microcircuit resulted in sleep reduction and fragmentation. n = 36-40. (B) Simultaneous silence of PAM-α1-DPM microcircuit without starvation had little effect on sleep and the number of sleep episodes. n = 29-31. (C) Sleep profiles of before, during and after activation of PAM-α1 neurons till supposed 24 h memory test with/without 0.1 mM gaboxadol (THIP) treatment. Application of THIP rescued sleep reduction induced by activation of PAM-α1 neurons. n = 38-42. (D-E) THIP rescued 24 h memory deficit induced by 1 h activation of PAM-α1 neurons during consolidation compared to genetic controls (D, n = 15-17) or compared to no THIP group (E, n = 17). (F) A working model of PAM-α1-DPM microcircuit in linking sleep and memory. Red filled circle: activated; blue filled circle: inactivated. See also Tables 1, 2 and 4.

Figure 1

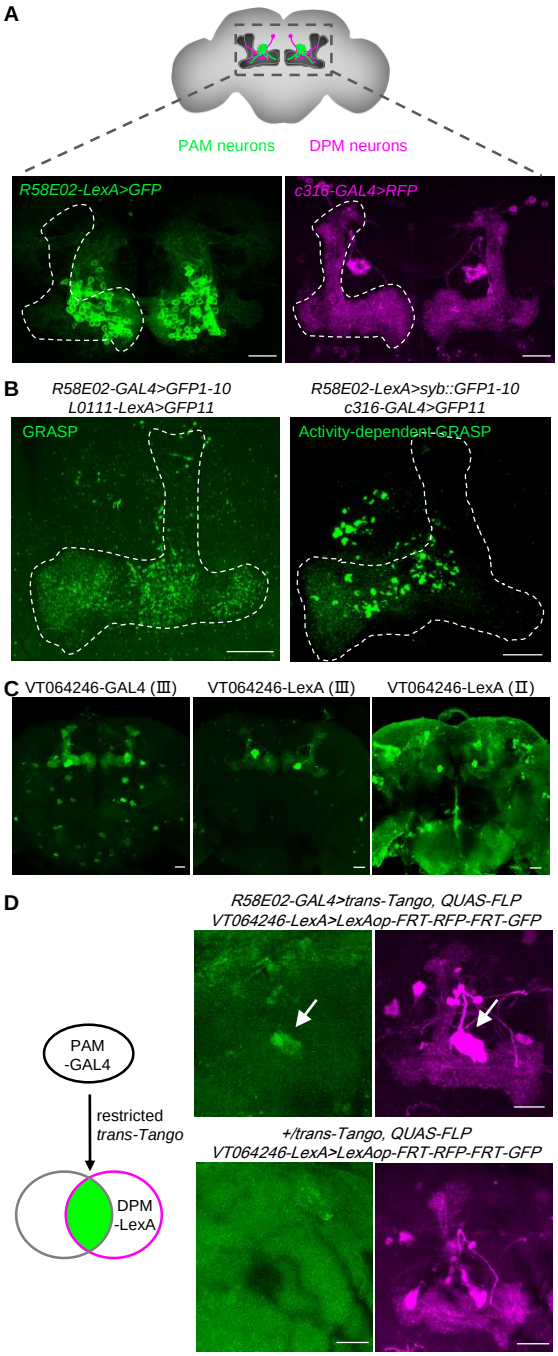
A
PAM neurons
DPM neurons
R58E02-LexA>GFP
c316-GAL4>RFP
B
R58E02-GAL4>GFP1-10
L0111-LexA>GFP11
R58E02-LexA>syb::GFP1-10
c316-GAL4>GFP11
GRASP
Activity-dependent-GRASP
C
VT064246-GAL4 (Ⅲ)
VT064246-LexA (Ⅲ)
VT064246-LexA (Ⅱ)
D
R58E02-GAL4>trans-Tango, QUAS-FLP
VT064246-LexA>LexAop-FRT-RFP-FRT-GFP
PAM
-GAL4
restricted
trans-Tango
DPM
-LexA
+/trans-Tango, QUAS-FLP
VT064246-LexA>LexAop-FRT-RFP-FRT-GFP

Figure 2

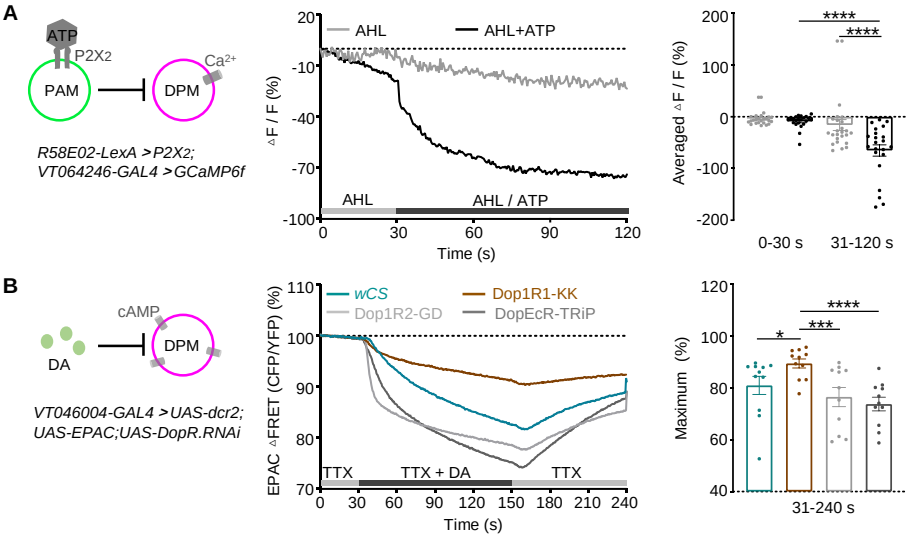
A
ATP
P2X2
Ca2+
PAM
DPM
R58E02-LexA >P2X2;
VT064246-GAL4 >GCaMP6f
AHL
AHL+ATP
ΔF / F (%)
AHL
AHL / ATP
Time (s)
Averaged ΔF / F (%)
****
****
0-30 s
31-120 s
B
cAMP
DA
DPM
VT046004-GAL4 >UAS-dcr2;
UAS-EPAC;UAS-DopR.RNAi
wCS
Dop1R1-KK
Dop1R2-GD
DopEcR-TRiP
EPAC ΔFRET (CFP/YFP) (%)
TTX
TTX + DA
TTX
Time (s)
Maximum (%)
*
***
****
31-240 s

Figure 3

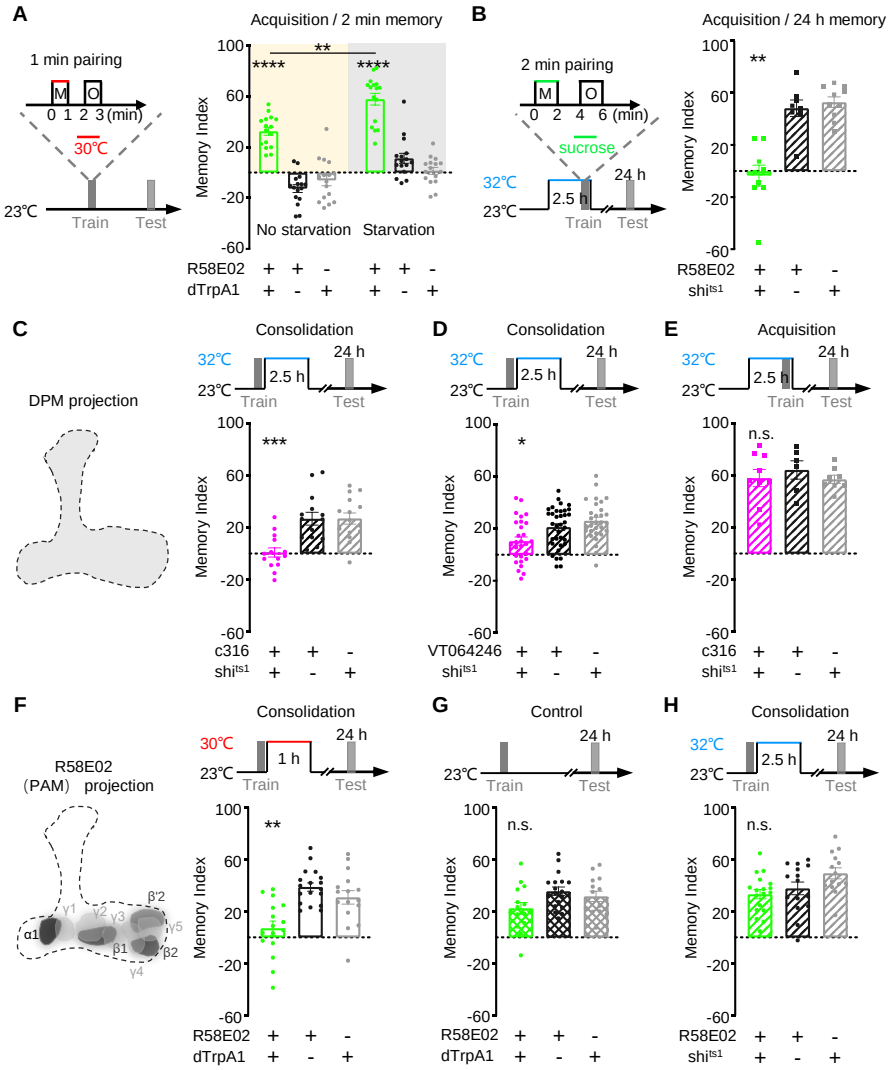
A
1 min pairing
M
O
0 1 2 3 (min)
30℃
23℃
Train
Test
Acquisition / 2 min memory
Memory Index
100
60
20
-20
-60
**
****
****
No starvation
Starvation
R58E02 + + - + + -
dTrpA1 + - + + - +
B
2 min pairing
M
O
0 2 4 6 (min)
sucrose
32℃
23℃
2.5 h
24 h
Train
Test
Acquisition / 24 h memory
Memory Index
**
R58E02 + + -
shi^ts1 + - +
C
DPM projection
Consolidation
32℃
23℃
2.5 h
24 h
Train
Test
Memory Index
***
c316 + + -
shi^ts1 + - +
D
Consolidation
32℃
23℃
2.5 h
24 h
Train
Test
Memory Index
*
VT064246 + + -
shi^ts1 + - +
E
Acquisition
32℃
23℃
2.5 h
24 h
Train
Test
Memory Index
n.s.
c316 + + -
shi^ts1 + - +
F
R58E02
(PAM) projection
α1
γ1
γ2
γ3
γ4
γ5
β1
β2
β'2
Consolidation
30℃
23℃
1 h
24 h
Train
Test
Memory Index
**
R58E02 + + -
dTrpA1 + - +
G
Control
23℃
24 h
Train
Test
Memory Index
n.s.
R58E02 + + -
dTrpA1 + - +
H
Consolidation
32℃
23℃
2.5 h
24 h
Train
Test
Memory Index
n.s.
R58E02 + + -
shi^ts1 + - +

Figure 4

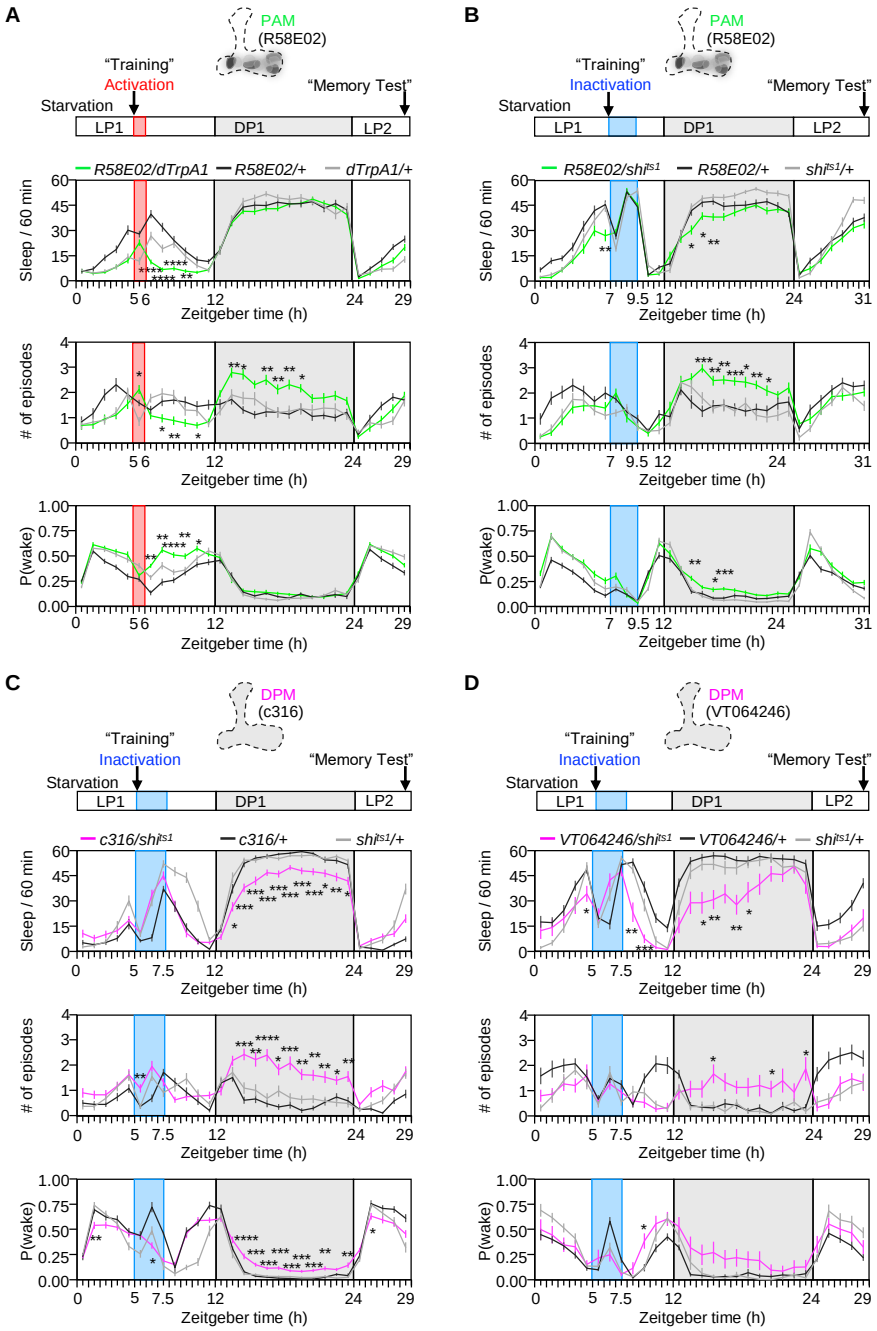
A
PAM
(R58E02)
"Training"
Activation
"Memory Test"
Starvation
LP1
DP1
LP2
R58E02/dTrpA1
R58E02/+
dTrpA1/+
Sleep / 60 min
# of episodes
P(wake)
Zeitgeber time (h)
B
PAM
(R58E02)
"Training"
Inactivation
"Memory Test"
Starvation
LP1
DP1
LP2
R58E02/shi^ts1
R58E02/+
shi^ts1/+
Sleep / 60 min
# of episodes
P(wake)
Zeitgeber time (h)
C
DPM
(c316)
"Training"
Inactivation
"Memory Test"
Starvation
LP1
DP1
LP2
c316/shi^ts1
c316/+
shi^ts1/+
Sleep / 60 min
# of episodes
P(wake)
Zeitgeber time (h)
D
DPM
(VT064246)
"Training"
Inactivation
"Memory Test"
Starvation
LP1
DP1
LP2
VT064246/shi^ts1
VT064246/+
shi^ts1/+
Sleep / 60 min
# of episodes
P(wake)
Zeitgeber time (h)

Figure 5

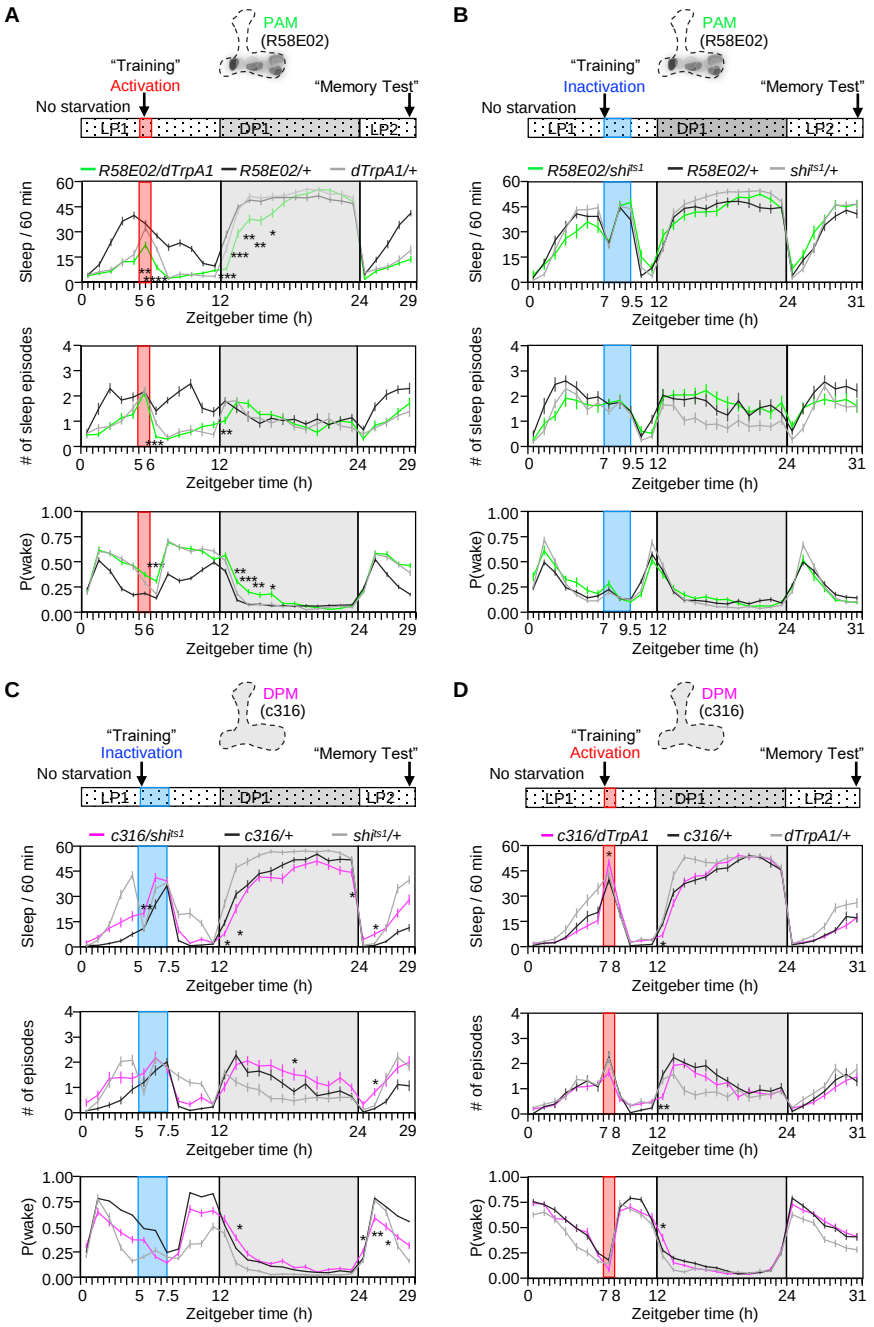
A
PAM
(R58E02)
"Training"
Activation
"Memory Test"
No starvation
LP1
DP1
LP2
R58E02/dTrpA1
R58E02/+
dTrpA1/+
Sleep / 60 min
# of sleep episodes
P(wake)
Zeitgeber time (h)
B
PAM
(R58E02)
"Training"
Inactivation
"Memory Test"
No starvation
R58E02/shi^ts1
R58E02/+
shi^ts1/+
C
DPM
(c316)
"Training"
Inactivation
"Memory Test"
c316/shi^ts1
c316/+
shi^ts1/+
# of episodes
D
DPM
(c316)
"Training"
Activation
"Memory Test"
c316/dTrpA1
c316/+
dTrpA1/+

Figure 6

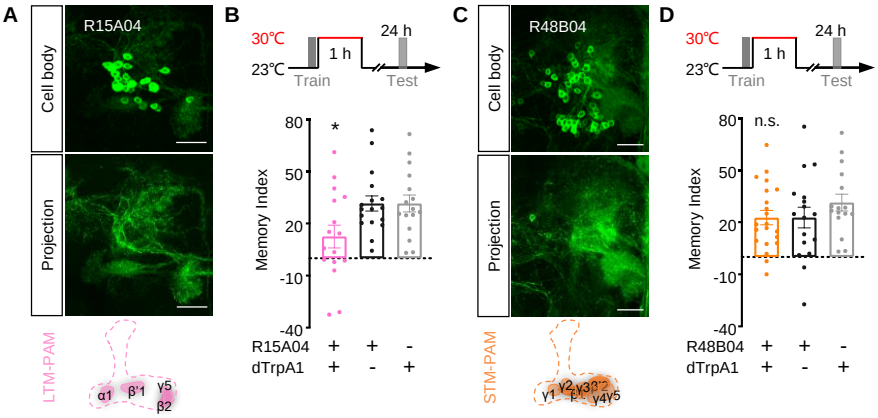

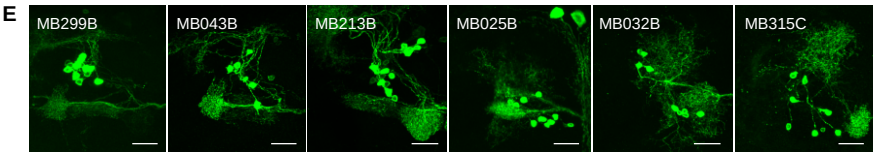

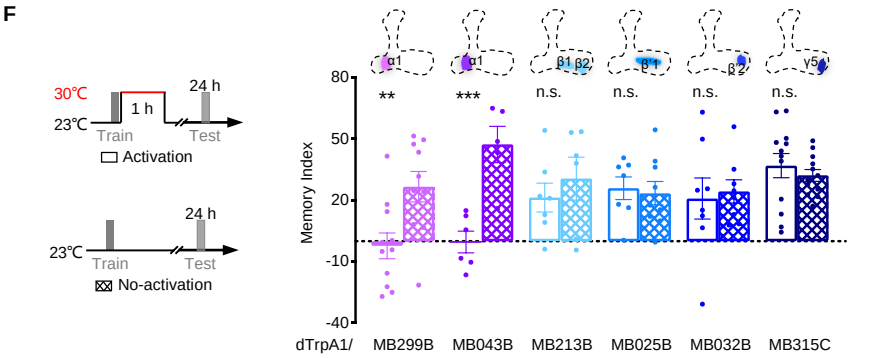

G

driver	# of cells / hemisphere	α1	β1	β2	β'1ap	β'1m
MB299B	12±5	+++	+	+	-	-
MB043B	6±2	++++	++	-	++	++

Figure 7

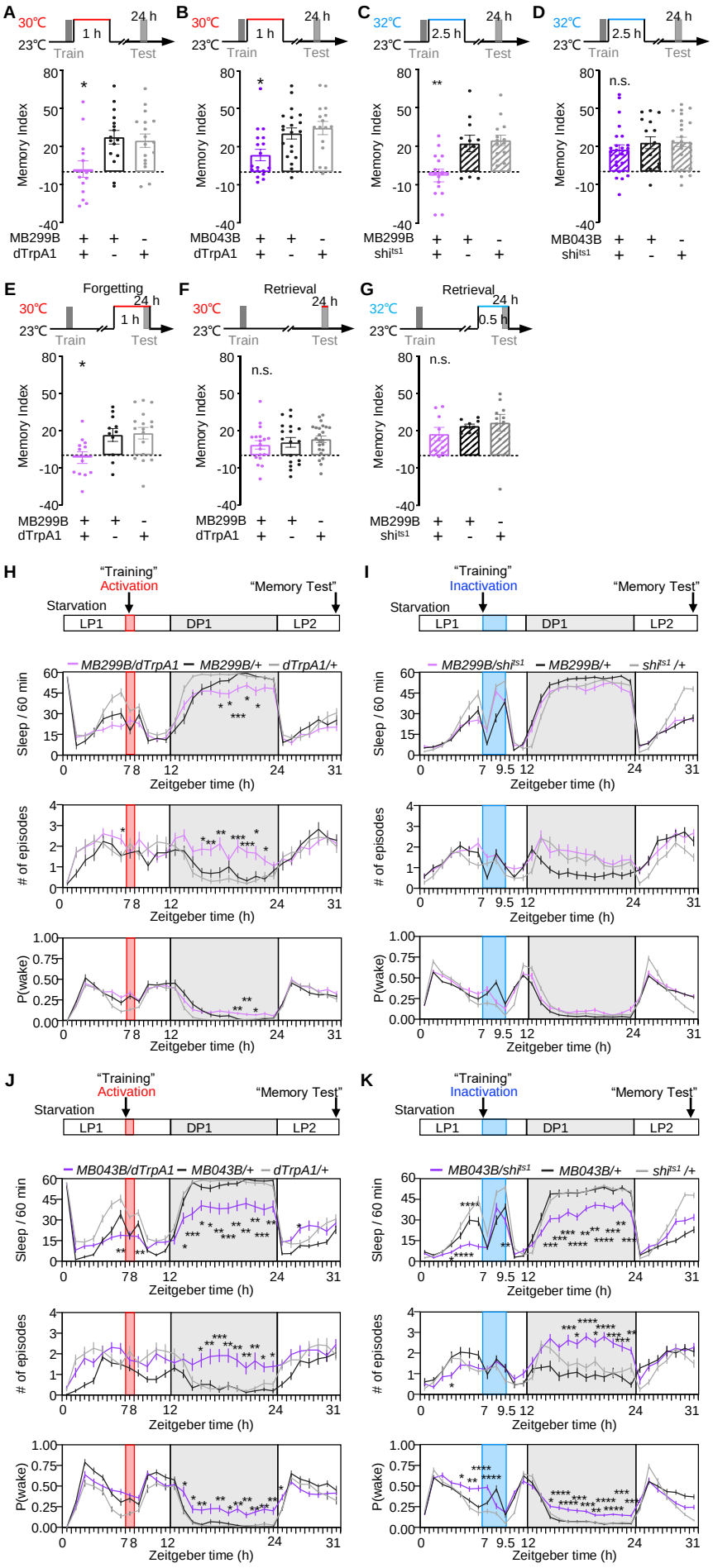
A
30℃
23℃
1 h
24 h
Train
Test
Memory Index
MB299B
dTrpA1
B
MB043B
C
32℃
2.5 h
shi^ts1
D
n.s.
E
Forgetting
F
Retrieval
G
0.5 h
H
"Training"
Activation
"Memory Test"
Starvation
LP1
DP1
LP2
MB299B/dTrpA1
MB299B/+
dTrpA1/+
Sleep / 60 min
Zeitgeber time (h)
# of episodes
P(wake)
I
Inactivation
MB299B/shi^ts1
shi^ts1 /+
J
MB043B/dTrpA1
MB043B/+
dTrpA1/+
K
MB043B/shi^ts1
shi^ts1 /+

Figure 8

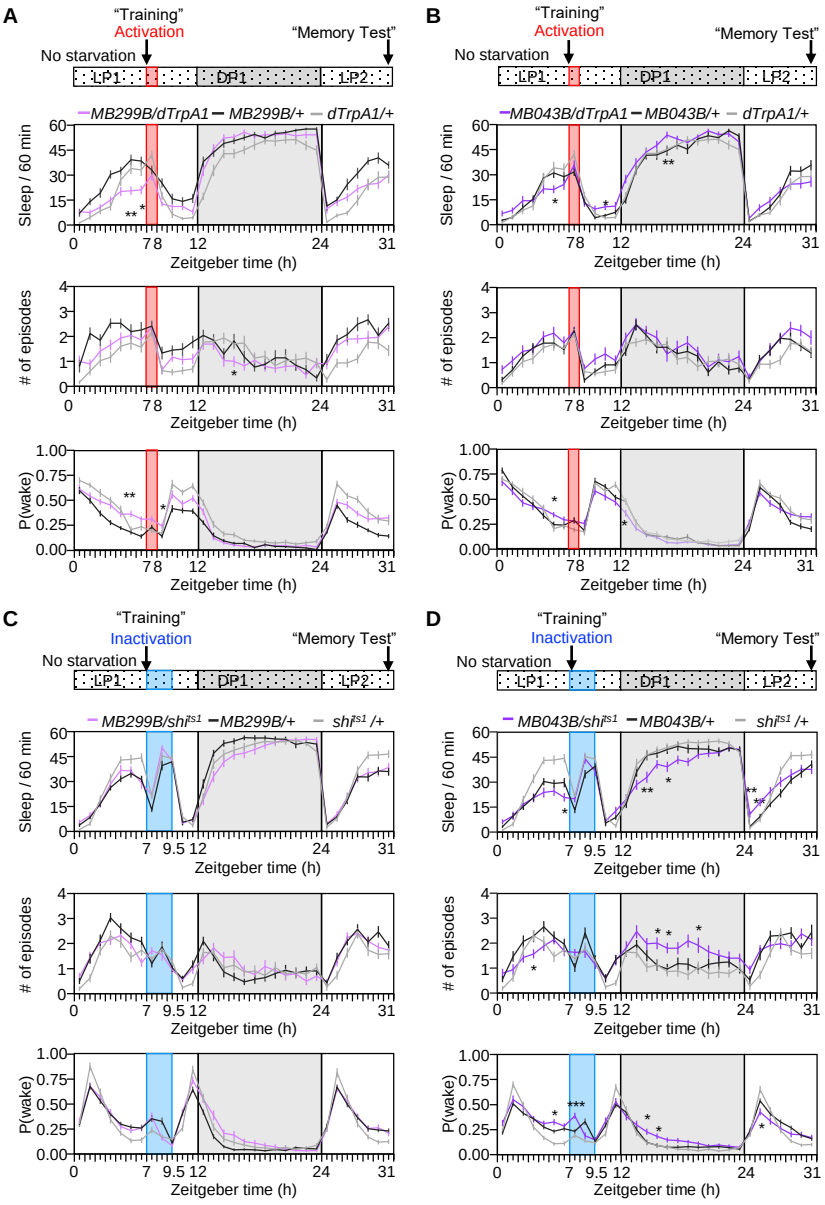
A
"Training"
Activation
"Memory Test"
No starvation
LP1
DP1
LP2
MB299B/dTrpA1
MB299B/+
dTrpA1/+
Sleep / 60 min
# of episodes
P(wake)
Zeitgeber time (h)
B
MB043B/dTrpA1
MB043B/+
dTrpA1/+
C
Inactivation
MB299B/shi^ts1
shi^ts1 /+
D
MB043B/shi^ts1

Figure 9

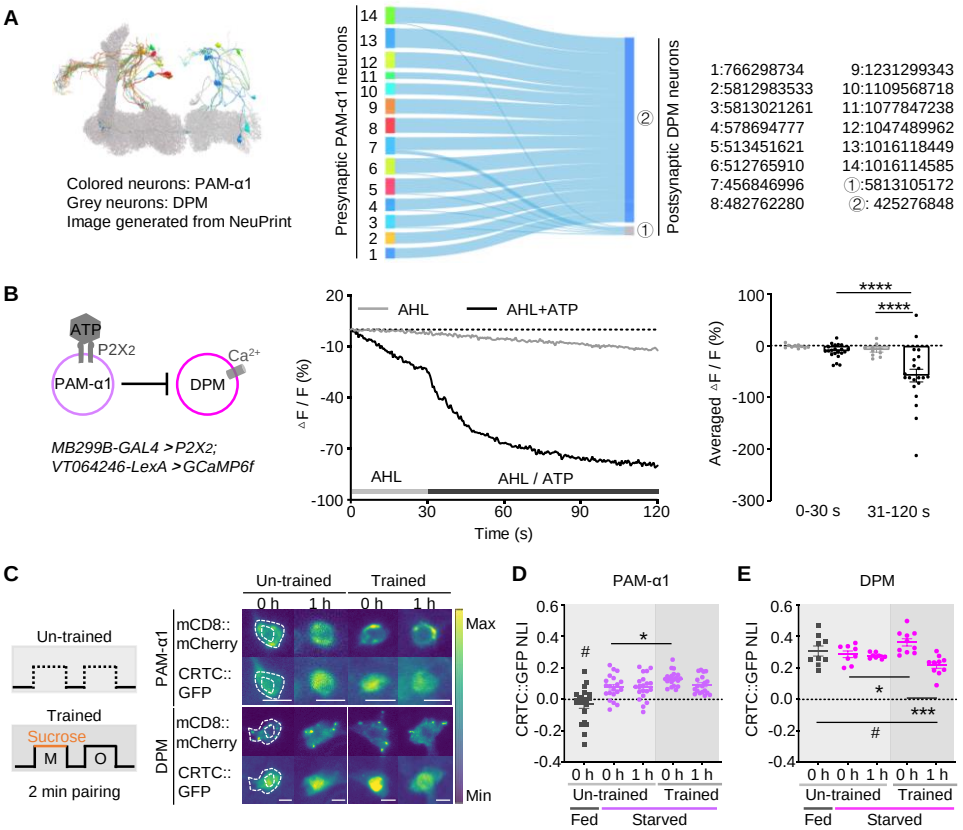
A
Colored neurons: PAM-α1
Grey neurons: DPM
Image generated from NeuPrint
Presynaptic PAM-α1 neurons
Postsynaptic DPM neurons
1:766298734
2:5812983533
3:5813021261
4:578694777
5:513451621
6:512765910
7:456846996
8:482762280
9:1231299343
10:1109568718
11:1077847238
12:1047489962
13:1016118449
14:1016114585
①:5813105172
②: 425276848
B
ATP
P2X2
PAM-α1
DPM
Ca2+
MB299B-GAL4 >P2X2;
VT064246-LexA >GCaMP6f
AHL
AHL+ATP
AHL / ATP
ΔF / F (%)
Time (s)
Averaged ΔF / F (%)
0-30 s
31-120 s
C
Un-trained
Trained
Sucrose
M
O
2 min pairing
PAM-α1
DPM
mCD8::mCherry
CRTC::GFP
Max
Min
D
PAM-α1
CRTC::GFP NLI
Un-trained
Trained
Fed
Starved
E
DPM

Figure 10

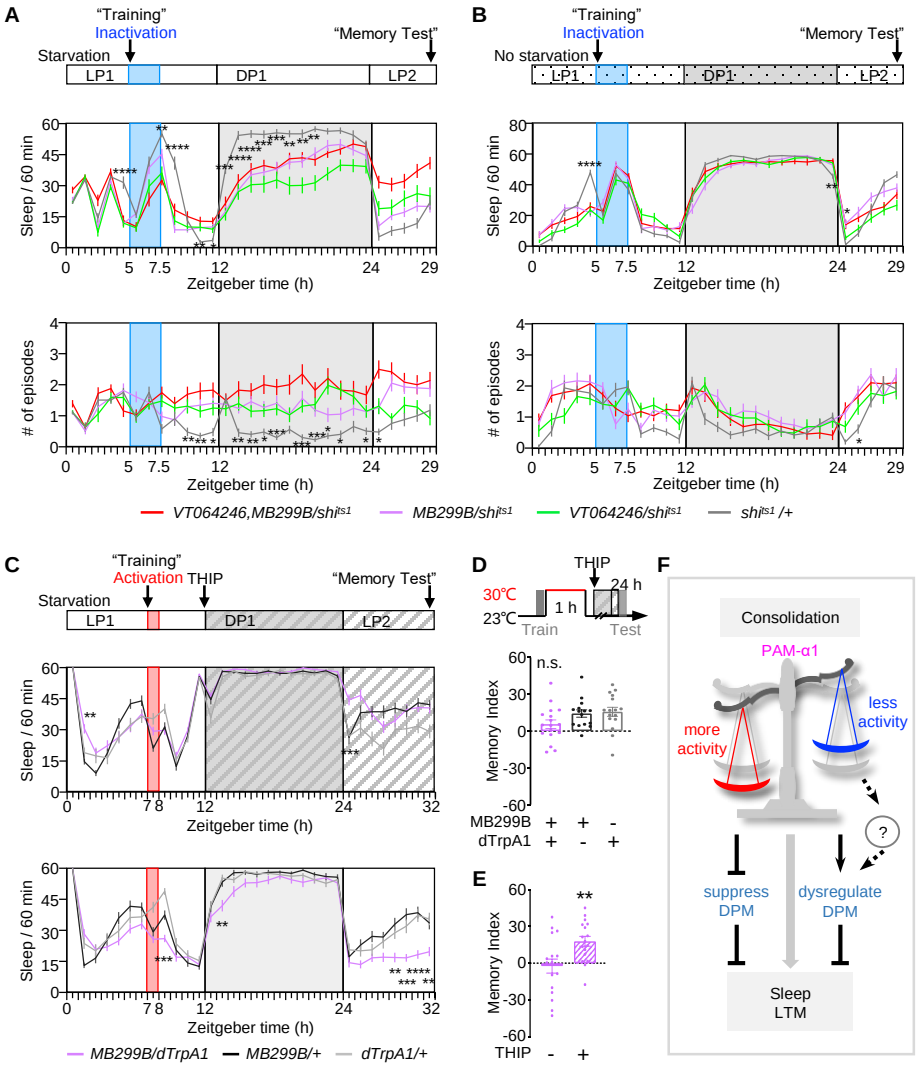
A
"Training"
Inactivation
Starvation
"Memory Test"
LP1
DP1
LP2
Sleep / 60 min
Zeitgeber time (h)
# of episodes
B
"Training"
Inactivation
No starvation
"Memory Test"
VT064246,MB299B/shi^{ts1}
MB299B/shi^{ts1}
VT064246/shi^{ts1}
shi^{ts1}/+
C
"Training"
Activation THIP
Starvation
"Memory Test"
MB299B/dTrpA1
MB299B/+
dTrpA1/+
D
THIP
24 h
30°C
23°C
1 h
Train
Test
n.s.
Memory Index
MB299B + + -
dTrpA1 + - +
E
THIP - +
F
Consolidation
PAM-α1
more activity
less activity
?
suppress DPM
dysregulate DPM
Sleep LTM